
QUANTIFYING SEASONAL HYDROGEN STORAGE DEMANDS UNDER COST AND MARKET UPTAKE UNCERTAINTIES IN ENERGY SYSTEM TRANSFORMATION PATHWAYS

A PREPRINT

✉ Felix Frischmuth¹, ✉ Mattis Berghoff¹, ✉ Martin Braun^{1,2}, and ✉ Philipp Härtel^{1,2}

¹Fraunhofer Institute for Energy Economics and Energy System Technology IEE, Joseph-Beuys-Str. 8, Kassel, 34117, Hessen, Germany

²Energy Management and Power System Operation, University of Kassel, 3Wilhelmshöher Allee 73, Kassel, 34121, Hessen, Germany

22nd April 2024

ABSTRACT

Climate neutrality paradigms put electricity systems at the core of a clean energy supply. At the same time, indirect electrification, with a potential uptake of hydrogen or derived fuel economy, plays a crucial role in decarbonising the energy supply and industrial processes. Besides energy markets coordinating the transition, climate and energy policy targets require fundamental changes and expansions in the energy transmission, import, distribution, and storage infrastructures. While existing studies identify relevant demands for hydrogen, critical decisions involve imports versus domestic fuel production and investments in new or repurposing existing pipeline and storage infrastructure. Linking the pan-European energy system planning model SCOPE SD with the multi-period European gas market model IMAGINE, the case study analysis and its transformation pathway results indicate extensive network development of hydrogen infrastructure, including expansion beyond refurbished methane infrastructure. However, the ranges of future hydrogen storage costs and market uptake restrictions expose and quantify the uncertainty of its role in Europe's transformation. The study finds that rapidly planning the construction of hydrogen storage and pipeline infrastructure is crucial to achieving the required capacity by 2050.

Keywords gas market model · hydrogen · renewable fuels · capacity expansion planning · energy system modelling

1 Introduction

Clean hydrogen (H₂) has assumed great importance under the REPowerEU strategy as part of the European Union's new energy security policy [1]. It plans an ambitious ramp-up of the H₂ economy in Europe over the next few years, both on Europe's consumer and producer side. Energy sovereignty is receiving increased attention, which implies less import of fossil energy sources and a diverse import mix of renewable-based fuels such as green H₂. The European Commission accelerates its progress towards Europe becoming the first climate-neutral continent [2]. To that end, implementing a trans-European energy network is a key element as well as other parts of an infrastructure required for renewable fuels, including new and repurposed H₂ pipeline networks and large-scale electrolyser and storage facilities [3].

The following article focuses on the demands for H₂ storage as a critical element for providing Europe's energy security in the clean transition. The model-based approach analyses the interactions of an integrated pan-European power and energy system with the trans-European energy infrastructure investments in H₂ storage and pipeline networks.

1.1 Previous work

Recent studies identify significant H₂ demands in deep decarbonisation pathways for Europe, see e.g. [4], and highlight cost benefits from integrated planning of electricity and gas infrastructure and markets, see e.g. [5]. While many studies focus on H₂ transport within Europe, e.g. [4, 6, 5, 7], future needs for large-scale H₂ storage have received less attention in the recent literature.

Studies on the H₂ storage potential exhibit considerable theoretical potentials in salt caverns. The work in [8] indicates a large but unevenly distributed theoretical potential across Europe. The analysis in [4] determines relevant H₂ storage demands, but does not explicitly include them in the optimisation procedure of the underlying planning problem. While a need for seasonal storage is identified, see e.g. [9], it remains much lower than today's demands for methane (CH₄) storage. The studies in [5], [10], and [11] also point to the importance of H₂ storage for the design of a future European H₂ infrastructure but focus their analysis on other market and system components. Furthermore, the models either work with a coarser temporal resolution and less precise regional data or consider a single planning period or year instead of a path-dependent transition.

1.2 Uncertainty of gas storage demands

Analysing the increasing coordination of power and gas markets in net-neutral systems requires high temporal granularity, pathway-dependent multi-period analysis, interacting H₂ and CH₄ infrastructure, and multiple sourcing strategies, which have not been the focus of previous models. The main contributions of this work include the following:

- path-dependent investment decisions for H₂ and CH₄ infrastructure components as well as system operation decisions of H₂ and CH₄ markets in Europe;
- analysis of trade-off between storage and pipeline in Europe's transition to climate neutrality;
- coupling of electricity and H₂ markets on a European and global scale with the established energy system planning framework SCOPE SD;
- transformation path results for a combination of storage cost uncertainties and market growth variations on European and country level.

The remainder is organised as follows. Section 2 explains the model linking approach and shows a detailed formulation of the IMAGINE framework and the model improvements. Section 3 sets up the case study's structure and assumptions for analysing gas sector transformations towards a carbon-neutral Europe. Section 4 presents and discusses the optimisation model results. Section 5 closes with a summary and draws relevant conclusions.

2 Methodology

2.1 Conceptual approach

The methodology follows the approach described in [12], which involves the pan-European cross-sectoral capacity expansion planning framework SCOPE SD (Scenario Development). We refer to [13, 14, 15, 16, 17] for recent formulations and applications. The energy system model SCOPE SD is combined with the market-based expansion planning framework IMAGINE (Infrastructure and market transformations for Gas in Europe). Linking those two models involves sectoral H₂ and CH₄ demands, hourly H₂ and CH₄ demand profiles, and H₂ production schedules from domestic electrolysers, all endogenous and consistent results of the pan-European SCOPE SD instances. Figure 1 illustrates the methodology and how both model frameworks are linked in this approach.

Here, we perform one iteration between the two planning models, i.e. SCOPE SD develops a scenario pathway that IMAGINE uses as input. The sensitivity analysis involves input parameter variations for the IMAGINE model.

2.2 IMAGINE model

While SCOPE SD uses only a simplified representation of gas and fuel infrastructure developments, IMAGINE fills that gap by explicitly focusing on production, transport, and storage developments, given the low-carbon transition pathways involving domestic production and renewable import possibilities. To that end, IMAGINE uses structural and time-series data inputs to minimise all costs incurred for the investment and operation of pipelines, storage facilities, and terminals, as well as the import and domestic production of renewable and low-carbon fuels. The IMAGINE framework is a bottom-up techno-economic system model that makes deterministic multi-period capacity expansion

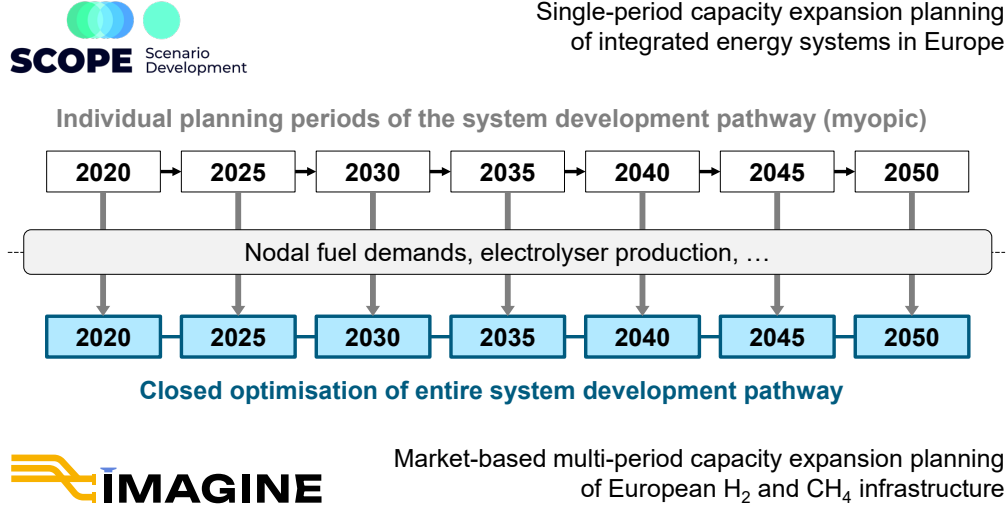


Figure 1: Linking of the single-period integrated energy system model SCOPE SD and the multi-period gas market and infrastructure planning model IMAGINE, own illustration.

and system operation decisions for a scenario pathway. Currently, each country is represented by one node, and the system operation formulations correspond to economic dispatch problems. Besides national day-ahead H₂ and CH₄ markets that are integrated through cross-border exchange, the model captures different national and global H₂ and CH₄ production options. By modelling national and pan-European markets, supply decision options include fossil fuels or synthetic renewable energy carriers imported or produced domestically. The modelling framework further allows the implementation of policy targets and instruments.

The IMAGINE framework is formulated as a linear programming (LP) optimisation model in the Python-based Pyomo package [18, 19] and developed as a multi-period decision model to account for pathway dependencies. In addressing the complexities of the European gas infrastructure transformation, the model adopts a simplified model for gas transport, specifically omitting the intricacies of linepacking, and utilises a coarser temporal modelling resolution, i.e. daily instead of hourly clearing. The methodological choice is driven by the need to maintain computational tractability when analysing the system-wide dynamics of storage, pipelines, and imports in a multi-period transformation pathway. Using a coarser temporal and technical resolution in our modelling approach, we focus on the long-term strategic development of the gas infrastructure. The approach is deemed adequate for capturing the essential interactions and trends at a pan-European level, which is crucial for guiding strategic decisions and policy formulation.

Based on the set definitions in the nomenclature, the model formulation features different parts for the components representing fuel production, pipelines, storage systems, the implemented markets and instruments, and finally, the objective function. Note that all decision variables are defined as non-negative reals unless stated otherwise.

Nomenclature

Sets and indices

Γ, γ Set of planning periods, indexed by γ

$\# \gamma$ Two-dimensional set of investment and operational planning period combinations, indexed by $\gamma = (\gamma^{\text{inv}}, \gamma^{\text{op}})$

$\mathcal{A}^{\text{CH}_4/\text{H}_2}, a$ Set of two-dimensional tuples for CH₄/H₂ pipelines between nodes (directed/undirected arcs), indexed by a

\mathcal{I}, i Set of nodes, indexed by i

$\mathcal{S}_i^{\text{CH}_4/\text{H}_2}, s$ Set of CH₄/H₂ storage facilities at node i , indexed by s

\mathcal{T}_γ, t Set of time steps for $\gamma \in \Gamma$, $\mathcal{T}_\gamma = \{t_1, \dots, t_T\}$, indexed by t

$\mathcal{T}\mathcal{E}_i^{\text{CH}_4/\text{H}_2}, te$ Set of CH₄/H₂ terminal facilities at node i , indexed by te

BH_i Set of blue H₂ production facilities at node i , $BH_i \subseteq NG_i$

BIO_i, g Set of biomethane production facilities at node i , indexed by g

- $DOM_{i,g}$ Set of domestic hydrogen production facilities at node i , indexed by g
 $GH_{i,g}$ Set of green H₂ production facilities at node i , indexed by g
 $GY_{i,g}$ Set of grey H₂ production facilities at node i , indexed by g
 $NG_{i,g}$ Set of natural gas production facilities at node i , indexed by g
 $SNG_{i,g}$ Set of SNG production facilities at node i , $SNG_i \subseteq GH_i$, indexed by g

Parameters

- Δ_γ Years per planning period
 Δ_t Years per time step
 η_s^{in} Injection losses of natural gas storages at storage s
 η_s^{wd} Withdrawal losses of natural gas storages at storage s
 κ_s Storage self-discharge losses between individual time step at storage s
 κ_s^{IN} Ratio of maximal injection rate to volume of storage s
 κ_s^{WD} Ratio of maximal withdrawal rate to volume of storage s
 λ_s Self-discharge rate of natural gas storages at storage s
 $\overline{P}_{a,0}^{\text{CH}_4}$ Existing CH₄ pipeline capacity
 $\overline{SV}_{s,0}^{\text{CH}_4}$ Existing CH₄ storage capacity
 $\overline{TV}_{te,0}^{\text{CH}_4}$ Existing LNG terminal capacity
 $AV_{s,t,\gamma}$ Time-dependent availability factor
 $B_\gamma^{\text{CO}_2}$ CO₂ emission budget per period
 $C_{,\gamma}^{\text{op}}$ Operational costs parameter for pipelines/storage/terminals
 $C_{a,\gamma}^{(\cdot)}$ Lifetime Investment/Repurposing/Decommissioning/ costs parameter for pipelines/storage/terminal
 $D_{i,t,\gamma}^{(\cdot)}$ CH₄/H₂ demand
 $EF_g^{(\cdot)}$ CH₄/blue hydrogen/grey hydrogen/LNG emission factor
 $G_{g,t,\gamma}^{(\cdot)}$ Biomethane or domestic H₂ production
 GR Market growth rate
 MC_g synthetic natural gas (SNG) methanation conversion factor
 MIN_s Minimal storage level at storage s
 $PR_{a,\gamma}^{\text{inv}}$ Investment restriction for pipelines
 RC_g Steam reforming conversion parameter for blue H₂
 RF_a Effective repurposing factor
 RF_{te} Reforming conversion parameter for LH₂ terminals at terminal te
 $SR_{s,\gamma}^{\text{inv}}$ Investment restriction for storage
 $TLF_a^{(\cdot)}$ Distance-specific losses for CH₄/H₂ pipelines
 $V_{g,\gamma}^{(\cdot)}$ Annual natural gas/green hydrogen and SNG production volume

Decision variables

- $\overline{p}_{a,\gamma}^{(\cdot)\downarrow}$ Decommissioned CH₄/H₂ pipeline capacity
 $\overline{p}_{a,\gamma}^{(\cdot),\text{rep}(\cdot)}$ Repurposed pipeline capacity
 $\overline{p}_{a,\gamma}^{(\cdot)\uparrow}$ Newly-built CH₄/H₂ pipeline capacity
 $\overline{p}_{a,\gamma}^{(\cdot)}$ Available CH₄/H₂ pipeline capacity
 $\overline{sv}_{s,\gamma}^{(\cdot)\downarrow}$ Decommissioned CH₄/H₂ storage capacity

$\overline{sv}_{s,\gamma}^{(\cdot),\text{rep}(\cdot)}$	Repurposed storage capacity
$\overline{sv}_{s,\gamma}^{(\cdot)\uparrow}$	Newly-built CH ₄ /H ₂ storage capacity
$\overline{sv}_{s,\gamma}^{(\cdot)}$	Available CH ₄ /H ₂ storage capacity
$\overline{tv}_{te,\gamma}^{(\cdot)\downarrow}$	Decommissioned CH ₄ /H ₂ terminal capacity
$\overline{tv}_{te,\gamma}^{(\cdot),\text{rep}(\cdot)}$	Repurposed terminal capacity
$\overline{tv}_{te,\gamma}^{(\cdot)\uparrow}$	Newly-built CH ₄ /H ₂ terminal capacity
$\overline{tv}_{te,\gamma}^{(\cdot)}$	Available CH ₄ /H ₂ terminal capacity
$bh_{g,t,\gamma}$	Blue H ₂ production
$gf_{i,t,\gamma}$	Natural gas flare
$gh_{g,t,\gamma}$	Green H ₂ production
$gy_{g,t,\gamma}$	Grey hydrogen production
$lh_{g,t,\gamma}$	LH ₂ import
$ln_{g,t,\gamma}$	liquid natural gas (LNG) import
$ng_{g,t,\gamma}$	Natural gas generation
$p_{s,t,\gamma}^{(\cdot),\text{in}}$	CH ₄ /H ₂ injection volume
$p_{s,t,\gamma}^{(\cdot),\text{wd}}$	CH ₄ /H ₂ withdrawal volume
$p_{a=(i,j),t,\gamma}^{(\cdot)}$	The unidirectional CH ₄ /bidirectional H ₂ flows from nodes $i \rightarrow j$
$sl_{s,t,\gamma}$	Storage level
$sn_{g,t,\gamma}$	SNG production

2.2.1 Preliminary definitions

Before going into the mathematical formulations for the system components, we define the following sets and mapping functions to allow for concise model formulations:

$$[k]_j := \begin{cases} \{k, \dots, j\}, & \text{if } j \geq k \\ \emptyset, & \text{if } j < k \end{cases}, \quad (1a)$$

$$\mathbb{I}^{\text{dec}} := \{(\gamma^{\text{inv}}, \gamma^{\text{op}}) \in \Gamma \times \Gamma \mid \gamma^{\text{op}} > \gamma^{\text{inv}} \wedge \gamma^{\text{inv}} > 1\}, \quad (1b)$$

$$\mathbb{I}^{\text{rep}} := \{(\gamma^{\text{inv}}, \gamma^{\text{op}}) \in \Gamma \times \Gamma \mid \gamma^{\text{op}} > \gamma^{\text{inv}}\}, \quad (1c)$$

$$\delta^{\text{CH}_4}(a) := \{(i, j) \in \mathcal{A}^{\text{CH}_4} \mid a = (i, j) \vee a = (j, i)\}, \quad (1d)$$

$$\delta^{\text{out}}(i, \mathcal{A}) := \{a \in \mathcal{A} \mid \exists j \text{ with } a = (i, j)\}, \quad (1e)$$

$$\delta^{\text{in}}(i, \mathcal{A}) := \{a \in \mathcal{A} \mid \exists j \text{ with } a = (j, i)\}, \quad (1f)$$

where Equation (1a) defines index lists to map the corresponding multi-period capacity expansion, repurposing, and decommissioning decisions, Equations (1b) and (1c) define two-dimensional index sets to map the decommissioning and repurposing decisions, Equation (1d) maps unidirectional CH₄ pipelines to bidirectional H₂ arcs, and Equations (1e) and (1f) define the out- and inflowing arcs for nodal commodity balances.

2.2.2 Fuel production

The natural gas generation $ng_{g,t,\gamma}$ is limited by the planning period's, e.g. annual, energy production volume $V_{g,\gamma}^{\text{CH}_4}$. If a facility is viable for blue H₂ production $bh_{g,t,\gamma}$, the combined production quantities are limited by that volume, taking the blue H₂ reforming conversion parameter $RC_g \in [0, 1]$ into account. The corresponding constraint writes as follows $\forall g \in NG_i, \forall i \in \mathcal{I}, \forall \gamma \in \Gamma$:

$$\sum_{t \in \mathcal{T}_\gamma} \left(ng_{g,t,\gamma} + \sum_{\substack{\bar{g} \in BH_i \\ \bar{g} = g}} \frac{bh_{\bar{g},t,\gamma}}{RC_{\bar{g}}} \right) \leq V_{g,\gamma}^{\text{CH}_4}. \quad (2)$$

The production of green H_2 $gh_{g,t,\gamma}$ and SNG $sn_{g,t,\gamma}$ are limited by the annual energy production volume $V_{g,\gamma}^{GH_2}$. The combined production quantities are limited by that volume, taking the SNG methanation conversion parameter $MC_g \in [0, 1]$ into account. The corresponding constraint writes as follows $\forall g \in GH_i, \forall i \in \mathcal{I}, \forall \gamma \in \Gamma$:

$$\sum_{t \in \mathcal{T}_\gamma} \left(gh_{g,t,\gamma} + \sum_{\substack{\bar{g} \in SNG_i \\ \bar{g}=g}} \frac{sn_{\bar{g},t,\gamma}}{MC_{\bar{g}}} \right) \leq V_{g,\gamma}^{GH_2}. \quad (3)$$

2.2.3 Pipelines

By explicitly accounting for cross-border exchange flows between bidding zones (nodes), the modelling framework represents market integration and coupling effects. The pipeline network representation assumes a simplified transport gas flow model and focuses on cross-border exchange, mostly ignoring network constraints arising within bidding zones. Flows are based on daily capacity values and neglect the gas flow equations, i.e. pressure drop and linepacking in pipeline segments [20].

Methane (CH₄) The available pipeline capacity $\bar{p}_{a,\gamma}^{CH_4}$ limits the unidirectional CH₄ flows $p_{a=(i,j),t,\gamma}^{CH_4}$ from nodes $i \rightarrow j$ as follows:

$$p_{a,t,\gamma}^{CH_4} \leq \bar{p}_{a,\gamma}^{CH_4} \quad \forall a \in \mathcal{A}^{CH_4}, \forall t \in \mathcal{T}_\gamma, \forall \gamma \in \Gamma. \quad (4a)$$

Capacity decisions for the available pipeline capacity are explicitly modelled for every planning period, so that $\forall a \in \mathcal{A}^{CH_4}$:

$$\bar{p}_{a,1}^{CH_4} = \bar{P}_{a,0}^{CH_4} + \bar{p}_{a,1}^{CH_4\uparrow} - \bar{p}_{a,(1,1)}^{CH_4.rep\downarrow}, \quad (4b)$$

$$\bar{p}_{a,\gamma^{op}}^{CH_4} = \bar{p}_{a,\gamma^{op}-1}^{CH_4} + \bar{p}_{a,\gamma^{op}}^{CH_4\uparrow} - \sum_{\gamma^{inv} \in [1]_{\gamma^{op}}} \bar{p}_{a,(\gamma^{inv},\gamma^{op})}^{CH_4.rep\downarrow} - \sum_{\gamma^{inv} \in [1]_{\gamma^{op}-1}} \bar{p}_{a,(\gamma^{inv},\gamma^{op})}^{CH_4\downarrow} \quad \forall \gamma^{op} \in \Gamma \setminus \{1\}, \quad (4c)$$

$$\bar{p}_{a,(1,\gamma^{op})}^{CH_4\downarrow} \leq \bar{P}_{a,0}^{CH_4} + \bar{p}_{a,1}^{CH_4\uparrow} - \sum_{\bar{\gamma}^{op} \in [2]_{\gamma^{op}-1}} \bar{p}_{a,(1,\bar{\gamma}^{op})}^{CH_4\downarrow} - \sum_{\bar{\gamma}^{op} = [1]_{\gamma^{op}}} \bar{p}_{a,(1,\bar{\gamma}^{op})}^{CH_4.rep\downarrow} \quad \forall \gamma^{op} \in \Gamma \setminus \{1\}, \quad (4d)$$

$$\bar{p}_{a,(\gamma^{inv},\gamma^{op})}^{CH_4\downarrow} \leq \bar{p}_{a,\gamma^{inv}}^{CH_4\uparrow} - \sum_{\bar{\gamma}^{op} \in [\gamma^{inv}+1]_{\gamma^{op}-1}} \bar{p}_{a,(\gamma^{inv},\bar{\gamma}^{op})}^{CH_4\downarrow} - \sum_{\bar{\gamma}^{op} = [\gamma^{inv}]_{\gamma^{op}}} \bar{p}_{a,(\gamma^{inv},\bar{\gamma}^{op})}^{CH_4.rep\downarrow} \quad \forall (\gamma^{inv}, \gamma^{op}) \in \Xi^{dec}. \quad (4e)$$

Here, Equation (4b) describes the pipeline capacity for CH₄ in the first planning period, which is determined by the existing $\bar{P}_{a,0}^{CH_4}$, the newly-built $\bar{p}_{a,1}^{CH_4\uparrow}$, and the repurposed $\bar{p}_{a,(1,\gamma^{op})}^{CH_4.rep\downarrow}$ (for H₂ transport) capacities in this planning period. Equation (4c) generalises Equation (4b) for the later planning periods, where previous decommissioning and repurposing decisions are taken into account for a given γ^{inv} . Equation (4d) limits the decommissioning of existing CH₄ pipeline capacities in the first planning period, and Equation (4e) limits the decommissioning of CH₄ pipeline capacities depending on the pre-existing capacity for all other planning periods. Note that capacities built in the last planning period cannot be decommissioned.

Hydrogen (H₂) The model can either build new H₂ or repurpose existing CH₄ pipelines. The corresponding capacity constraints are similar to Equations (4a) to (4e). Unlike CH₄ pipelines, however, H₂ pipelines are assumed to be built in both flow directions. Hence, cross-border H₂ flows between two nodes i and j can be bidirectional (undirected graph), and are limited by the corresponding installed capacities $\forall a \in \mathcal{A}^{H_2}, \forall t \in \mathcal{T}, \forall \gamma \in \Gamma$:

$$p_{(i,j),t,\gamma}^{H_2} + p_{(j,i),t,\gamma}^{H_2} \leq \bar{p}_{a,\gamma}^{H_2} \quad (i,j) = a. \quad (5a)$$

Decisions for the available H₂ pipeline capacity $\bar{p}_{a,\gamma}^{H_2}$ are explicitly modelled for every planning period γ , so that $\forall a \in \mathcal{A}^{H_2}$:

$$\bar{p}_{a,1}^{H_2} = \bar{P}_{a,0}^{H_2} + \bar{p}_{a,1}^{H_2\uparrow} + \bar{p}_{a,(1,1)}^{H_2.rep\uparrow}, \quad (5b)$$

$$\bar{p}_{a,\gamma^{op}}^{H_2} = \bar{p}_{a,\gamma^{op}-1}^{H_2} + \bar{p}_{a,\gamma^{op}}^{H_2\uparrow} + \sum_{\gamma^{inv} \in [1]_{\gamma^{op}}} \bar{p}_{a,(\gamma^{inv},\gamma^{op})}^{H_2.rep\uparrow} - \sum_{\gamma^{inv} \in [1]_{\gamma^{op}-1}} \bar{p}_{a,(\gamma^{inv},\gamma^{op})}^{H_2\downarrow} \quad \forall \gamma^{op} \in \Gamma \setminus \{1\},$$

$$\bar{p}_{a,(1,\gamma^{op})}^{H_2\downarrow} \leq \bar{P}_{a,0}^{H_2} + \bar{p}_{a,1}^{H_2\uparrow} + \sum_{\bar{\gamma}^{op} = [1]_{\gamma^{op}}} \bar{p}_{a,(1,\bar{\gamma}^{op})}^{H_2.rep\uparrow} - \sum_{\bar{\gamma}^{op} \in [2]_{\gamma^{op}-1}} \bar{p}_{a,(1,\bar{\gamma}^{op})}^{H_2\downarrow} \quad \forall \gamma^{op} \in \Gamma \setminus \{1\}, \quad (5c)$$

$$\bar{p}_{a,(\gamma^{inv}, \gamma^{op})}^{H_2\downarrow} \leq \bar{p}_{a, \gamma^{inv}}^{H_2\uparrow} + \sum_{\bar{\gamma}^{op}=[\gamma^{inv}]_{\gamma^{op}}} \bar{p}_{a,(\gamma^{inv}, \bar{\gamma}^{op})}^{H_2,rep\uparrow} - \sum_{\bar{\gamma}^{op} \in [\gamma^{inv}+1]_{\gamma^{op}-1}} \bar{p}_{a,(\gamma^{inv}, \bar{\gamma}^{op})}^{H_2\downarrow} \quad \forall (\gamma^{inv}, \gamma^{op}) \in \mathbb{N}^{\leq dec}, \quad (5d)$$

$$\bar{p}_{a, \gamma}^{H_2,rep\uparrow} = \sum_{\bar{a} \in \delta^{CH_4}(a)} RF_a \bar{p}_{\bar{a}, \gamma}^{CH_4,rep\downarrow} \quad \forall \gamma \in \mathbb{N}^{\leq rep}. \quad (5e)$$

Here, Equation (5b) determines the H_2 transport capacity for the first planning period, which is determined by the newly-built $\bar{p}_{a, \gamma^{inv}}^{H_2\uparrow}$, the repurposed $\bar{p}_{a,(\gamma^{inv}, \bar{\gamma}^{op})}^{H_2,rep\uparrow}$, and the decommissioned capacity $\bar{p}_{a, \gamma}^{H_2\downarrow}$. Similar to Equation (4c), Equation (5) generalises Equation (5b) for all later planning periods. Note that incorporating a pre-existing H_2 pipeline capacity $\bar{P}_{a,0}^{H_2}$ is an option, especially relevant if using the model with a planning horizon starting in planning periods already featuring substantial H_2 infrastructure. Equations (5c) and (5d) limit the decommissioned H_2 pipeline capacities. Equation (5e) describes the conversion of repurposed CH_4 to H_2 capacities $\bar{p}_{a,(\gamma^{inv}, \bar{\gamma}^{op})}^{H_2,rep\uparrow}$ based on a linear effective repurposing factor $RF_a \in [0, 1]$.

2.2.4 Storage

The model considers five different types of CH_4 storage components, namely aquifers, rock caverns, salt caverns, depleted fields, and others, of which only salt caverns can be repurposed for H_2 storage. While capacity expansion and repurposing decisions of gas storage facilities correspond to the pipeline modelling approach, the dispatch constraints differ. Capacity decisions for the storage (volume) capacity $\bar{sv}_{s, \gamma}^{CH_4}$ and $\bar{sv}_{s, \gamma}^{H_2}$ are explicitly modelled for every planning period, see Equations (6a) to (6d), (9) and (9a) to (9d).

Methane (CH_4) Decisions for the available CH_4 storage capacity $\bar{sv}_{s, \gamma^{op}}^{CH_4}$ are explicitly modelled for every planning period and $\forall s \in \mathcal{S}^{CH_4}$, the constraints are written as follows:

$$\bar{sv}_{s,1}^{CH_4} = \bar{SV}_{s,0}^{CH_4} + \bar{sv}_{s,1}^{CH_4\uparrow} - \bar{sv}_{s,(1,1)}^{CH_4,rep\downarrow}, \quad (6a)$$

$$\bar{sv}_{s, \gamma^{op}}^{CH_4} = \bar{sv}_{s, \gamma^{op}-1}^{CH_4} + \bar{sv}_{s, \gamma^{op}}^{CH_4\uparrow} - \sum_{\gamma^{inv} \in [1]_{\gamma^{op}}} \bar{sv}_{s,(\gamma^{inv}, \gamma^{op})}^{CH_4,rep\downarrow} - \sum_{\gamma^{inv} \in [1]_{\gamma^{op}-1}} \bar{sv}_{s,(\gamma^{inv}, \gamma^{op})}^{CH_4\downarrow} \quad \forall \gamma^{op} \in \Gamma \setminus \{1\}, \quad (6b)$$

$$\bar{sv}_{s,(1, \gamma^{op})}^{CH_4\downarrow} \leq \bar{SV}_{s,0}^{CH_4} + \bar{sv}_{s,1}^{CH_4\uparrow} - \sum_{\bar{\gamma}^{op}=[1]_{\gamma^{op}}} \bar{sv}_{s,(1, \bar{\gamma}^{op})}^{CH_4,rep\downarrow} - \sum_{\bar{\gamma}^{op} \in [2]_{\gamma^{op}-1}} \bar{sv}_{s,(1, \bar{\gamma}^{op})}^{CH_4\downarrow} \quad \forall \gamma^{op} \in \Gamma \setminus \{1\}, \quad (6c)$$

$$\bar{sv}_{s,(\gamma^{inv}, \gamma^{op})}^{CH_4\downarrow} \leq \bar{sv}_{s, \gamma^{inv}}^{CH_4\uparrow} - \sum_{\bar{\gamma}^{op}=[\gamma^{inv}]_{\gamma^{op}}} \bar{sv}_{s,(\gamma^{inv}, \bar{\gamma}^{op})}^{CH_4,rep\downarrow} - \sum_{\bar{\gamma}^{op} \in [\gamma^{inv}+1]_{\gamma^{op}-1}} \bar{sv}_{s,(\gamma^{inv}, \bar{\gamma}^{op})}^{CH_4\downarrow} \quad \forall (\gamma^{inv}, \gamma^{op}) \in \mathbb{N}^{\leq dec}, \quad (6d)$$

The operational constraints characterising the storage systems for CH_4 storage facilities, and they are written as follows $\forall s \in \mathcal{S}$, $\forall t \in \mathcal{T}$, $\forall \gamma \in \Gamma$:

$$p_{s,t,\gamma}^{CH_4,wd} \leq \bar{sv}_{s,\gamma} \kappa_s^{WD} AV_{s,t,\gamma}, \quad (7a)$$

$$p_{s,t,\gamma}^{CH_4,in} \leq \bar{sv}_{s,\gamma} \kappa_s^{IN} AV_{s,t,\gamma}, \quad (7b)$$

$$MIN_s \bar{sv}_{s,\gamma} AV_{s,t,\gamma} \leq sl_{s,t,\gamma} \leq \bar{sv}_{s,\gamma} AV_{s,t,\gamma}, \quad (7c)$$

$$sl_{s,t+1,\gamma} = sl_{s,t,\gamma} \kappa_s + \left(p_{s,t,\gamma}^{CH_4,in} \eta_s^{in} - \frac{p_{s,t,\gamma}^{CH_4,wd}}{\eta_s^{wd}} \right) \Delta_t, \quad (7d)$$

where Equations (7a) and (7b) limit the maximum storage withdrawal (wd) and injection (in) rates by the planning period-dependent capacities. Equation (7c) limits the storage level including a time-dependent availability parameter $AV_{s,t,\gamma}$ for aggregate maintenance and failure downtimes, and Equation (7d) denotes the intra-temporal gas storage continuity for every time step and planning period. Note that $\kappa_s = (1 - \lambda_s)$ accounts for the storage self-discharge losses between individual time steps and that the initial storage level is linked to the last considered time step per planning period $\forall s \in \mathcal{S}$, $\forall \gamma \in \Gamma$ by

$$sl_{s,t_1,\gamma} \leq sl_{s,t_T,\gamma} + \left(p_{s,t_T,\gamma}^{CH_4,in} \eta_s^{in} - \frac{p_{s,t_T,\gamma}^{CH_4,wd}}{\eta_s^{wd}} \right) \Delta_t. \quad (8)$$

Hydrogen (H₂) Decisions for the available H₂ storage capacity $\overline{sv}_{s,\gamma^{op}}^{\text{H}_2}$ are explicitly modelled for every planning period and written as follows $\forall s \in \mathcal{S}^{\text{H}_2}$.

$$\overline{sv}_{s,1}^{\text{H}_2} = \overline{SV}_{s,0}^{\text{H}_2} + \overline{sv}_{s,1}^{\text{H}_2\uparrow} + \overline{sv}_{s,(1,1)}^{\text{H}_2,\text{rep}\uparrow}, \quad (9a)$$

$$\overline{sv}_{s,\gamma^{op}}^{\text{H}_2} = \overline{sv}_{s,\gamma^{op}-1}^{\text{H}_2} + \overline{sv}_{s,\gamma^{op}}^{\text{H}_2\uparrow} + \sum_{\gamma^{\text{inv}} \in [1]_{\gamma^{op}}} \overline{sv}_{s,(\gamma^{\text{inv}},\gamma^{op})}^{\text{H}_2,\text{rep}\uparrow} - \sum_{\gamma^{\text{inv}} \in [1]_{\gamma^{op}-1}} \overline{sv}_{s,(\gamma^{\text{inv}},\gamma^{op})}^{\text{H}_2\downarrow} \quad \forall \gamma^{op} \in \Gamma \setminus \{1\},$$

$$\overline{sv}_{s,(1,\gamma^{op})}^{\text{H}_2\downarrow} \leq \overline{SV}_{s,0}^{\text{H}_2} + \overline{sv}_{s,1}^{\text{H}_2\uparrow} + \sum_{\bar{\gamma}^{op} \in [1]_{\gamma^{op}}} \overline{sv}_{s,(1,\bar{\gamma}^{op})}^{\text{H}_2,\text{rep}\uparrow} - \sum_{\bar{\gamma}^{op} \in [2]_{\gamma^{op}-1}} \overline{sv}_{s,(1,\bar{\gamma}^{op})}^{\text{H}_2\downarrow} \quad \forall \gamma^{op} \in \Gamma \setminus \{1\}, \quad (9b)$$

$$\overline{sv}_{s,(\gamma^{\text{inv}},\gamma^{op})}^{\text{H}_2\downarrow} \leq \overline{sv}_{s,\gamma^{\text{inv}}}^{\text{H}_2\uparrow} + \sum_{\bar{\gamma}^{op} \in [\gamma^{\text{inv}}]_{\gamma^{op}}} \overline{sv}_{s,(\gamma^{\text{inv}},\bar{\gamma}^{op})}^{\text{H}_2,\text{rep}\uparrow} - \sum_{\bar{\gamma}^{op} \in [\gamma^{\text{inv}}+1]_{\gamma^{op}-1}} \overline{sv}_{s,(\gamma^{\text{inv}},\bar{\gamma}^{op})}^{\text{H}_2\downarrow} \quad \forall (\gamma^{\text{inv}},\gamma^{op}) \in \leq^{\text{dec}}, \quad (9c)$$

$$\overline{sv}_{s,(\gamma^{\text{inv}},\gamma^{op})}^{\text{H}_2,\text{rep}\uparrow} = RF_s \overline{sv}_{s,(\gamma^{\text{inv}},\gamma^{op})}^{\text{CH}_4,\text{rep}\downarrow} \quad \forall \gamma \in \leq^{\text{rep}}. \quad (9d)$$

The operational constraints characterising the H₂ storage facilities are written as follows $\forall s \in \mathcal{S}, \forall t \in \mathcal{T}, \forall \gamma \in \Gamma$:

$$p_{s,t,\gamma}^{\text{H}_2,\text{wd}} \leq \overline{sv}_{s,\gamma} \kappa_s^{\text{WD}} AV_{s,t,\gamma}, \quad (10a)$$

$$p_{s,t,\gamma}^{\text{H}_2,\text{in}} \leq \overline{sv}_{s,\gamma} \kappa_s^{\text{IN}} AV_{s,t,\gamma}, \quad (10b)$$

$$\text{MIN}_s \overline{sv}_{s,\gamma} AV_{s,t,\gamma} \leq sl_{s,t,\gamma} \leq \overline{sv}_{s,\gamma} AV_{s,t,\gamma}, \quad (10c)$$

$$sl_{s,t+1,\gamma} = sl_{s,t,\gamma} \kappa_s + \left(p_{s,t,\gamma}^{\text{H}_2,\text{in}} \eta_s^{\text{in}} - \frac{p_{s,t,\gamma}^{\text{H}_2,\text{wd}}}{\eta_s^{\text{wd}}} \right) \Delta_t, \quad (10d)$$

where Equations (10a) and (10b) limit the maximum storage withdrawal (wd) and injection (in) rates by the planning period-dependent capacities. Equation (10c) limits the storage level including a time-dependent availability parameter $AV_{s,t,\gamma}$ for aggregate maintenance and failure downtimes, and Equation (10d) denotes the intra-temporal gas storage continuity for every time step and planning period. Note that $\kappa_s = (1 - \lambda_s)$ accounts for the storage self-discharge losses between individual time steps and that the initial storage level is linked to the last considered time step per planning period $\forall s \in \mathcal{S}, \forall \gamma \in \Gamma$ by

$$sl_{s,t_1,\gamma} \leq sl_{s,t_T,\gamma} + \left(p_{s,t_T,\gamma}^{\text{H}_2,\text{in}} \eta_s^{\text{in}} - \frac{p_{s,t_T,\gamma}^{\text{H}_2,\text{wd}}}{\eta_s^{\text{wd}}} \right) \Delta_t. \quad (11)$$

2.2.5 Markets for CH₄, H₂, and CO₂

The market clearing constraints ensure that the demand and supply of CH₄ and H₂ are balanced for each time step. The market clearing mechanisms are formulated as follows $\forall i \in \mathcal{I}, \forall t \in \mathcal{T}, \forall \gamma \in \Gamma$:

$$\begin{aligned} D_{i,t,\gamma}^{\text{CH}_4} &= \sum_{g \in \text{NG}_i} ng_{g,t,\gamma} + \sum_{te \in \mathcal{T}\mathcal{E}_i^{\text{CH}_4}} ln_{te,t,\gamma} + \sum_{g \in \text{SNG}_i} sn_{g,t,\gamma} - \sum_{g \in \text{GY}_i} \frac{gy_{g,t,\gamma}}{\text{RC}_g} + \sum_{g \in \text{BIO}_i} G_{g,t,\gamma}^{\text{BIO}} \\ &+ \sum_{s \in \mathcal{S}_i^{\text{CH}_4}} \left(p_{s,t,\gamma}^{\text{CH}_4,\text{wd}} - p_{s,t,\gamma}^{\text{CH}_4,\text{in}} \right) + \sum_{a \in \delta^{\text{in}}(i, \mathcal{A}^{\text{CH}_4})} p_{a,t,\gamma}^{\text{CH}_4} - \sum_{a \in \delta^{\text{out}}(i, \mathcal{A}^{\text{CH}_4})} p_{a,t,\gamma}^{\text{CH}_4} TLF_a^{\text{CH}_4} - gf_{i,t,\gamma} \end{aligned} \quad (12a)$$

$$\begin{aligned} D_{i,t,\gamma}^{\text{H}_2} &= \sum_{g \in \text{BH}_i} bh_{g,t,\gamma} + \sum_{g \in \mathcal{T}\mathcal{E}_i^{\text{H}_2}} lh_{te,t,\gamma} + \sum_{g \in \text{GH}_i} gh_{g,t,\gamma} + \sum_{g \in \text{GY}_i} gy_{g,t,\gamma} + \sum_{g \in \text{DOM}_i} G_{g,t,\gamma}^{\text{DOM}} + \\ &\sum_{s \in \mathcal{S}_i^{\text{H}_2}} \left(p_{s,t,\gamma}^{\text{H}_2,\text{wd}} - p_{s,t,\gamma}^{\text{H}_2,\text{in}} \right) + \sum_{a \in \delta^{\text{in}}(i, \mathcal{A}^{\text{H}_2})} p_{a,t,\gamma} - \sum_{a \in \delta^{\text{out}}(i, \mathcal{A}^{\text{H}_2})} p_{a,t,\gamma} TLF_a^{\text{H}_2}. \end{aligned} \quad (12b)$$

In Equation (12a), $D_{i,t,\gamma}^{\text{CH}_4}$ is the final (inelastic) CH₄ demand that needs to be covered together with the final (inelastic) biomethane production $G_{g,t,\gamma}^{\text{BIO}}$. In Equation (12b), $D_{i,t,\gamma}^{\text{H}_2}$ is the final (inelastic) H₂ demand that needs to be covered together with the final (inelastic) domestic H₂ production $G_{g,t,\gamma}^{\text{DOM}}$, which can consist of an onshore and offshore part. In case the desired CO₂ emission instruments include an emission budget and not (only) a price, a separate market is considered $\forall \gamma \in \Gamma$:

$$B_{\gamma}^{\text{CO}_2} \geq \sum_{t \in \mathcal{T}} \sum_{i \in \mathcal{I}} \left(\sum_{g \in \text{NG}_i} ng_{g,t,\gamma} EF_g^{\text{CH}_4} + \sum_{g \in \text{BH}_i} bh_{g,t,\gamma} EF_g^{\text{BH}} + \sum_{g \in \text{GH}_i} gh_{g,t,\gamma} EF_g^{\text{GH}} + \sum_{g \in \mathcal{T}\mathcal{E}_i^{\text{CH}_4}} ln_{g,t,\gamma} EF_g^{\text{LNG}} \right),$$

where $B_\gamma^{\text{CO}_2}$ represents the CO₂ emission budget per planning period. The system operation decisions must adhere to the planning period-specific budgets.

Note that Table 2 contains investment and fixed operation costs for new CH₄ pipelines, new H₂ pipelines and retrofit H₂ pipelines.

2.3 Model improvement for liquid energy carriers

To account for the infrastructure needs to import liquid carriers, the original model from [12] has been enhanced to include the possibility of building and decommissioning LNG and LH₂ terminals. In addition, existing LNG terminals can be repurposed for LH₂ use. The capacity expansion and repurposing decisions correspond to the pipeline modelling approach, see [12].

Methane (CH₄) The decisions for the terminal capacity $\overline{t}e_{s,\gamma}^{\text{CH}_4}$ and $\overline{t}e_{s,\gamma}^{\text{H}_2}$ are explicitly modelled for every planning period, see Equations (13a) to (13d), (15) and (15b) to (15d). Decisions for the available CH₄ terminal capacity $\overline{t}v_{te,\gamma^{\text{op}}}^{\text{CH}_4}$ are explicitly modelled for every planning period, so that $\forall te \in TE^{\text{CH}_4}, \forall i \in \mathcal{I}$:

$$\overline{t}v_{te,1}^{\text{CH}_4} = \overline{TV}_{te,0}^{\text{CH}_4} + \overline{t}v_{te,1}^{\text{CH}_4\uparrow} - \overline{t}v_{te,1}^{\text{CH}_4,\text{rep}\downarrow}, \quad (13a)$$

$$\overline{t}v_{te,\gamma^{\text{op}}}^{\text{CH}_4} = \overline{t}v_{te,\gamma^{\text{op}-1}}^{\text{CH}_4} + \overline{t}v_{te,\gamma^{\text{op}}}^{\text{CH}_4\uparrow} - \sum_{\gamma^{\text{inv}} \in [1]_{\gamma^{\text{op}}}} \overline{t}v_{te,(\gamma^{\text{inv}},\gamma^{\text{op}})}^{\text{CH}_4,\text{rep}\downarrow} - \sum_{\gamma^{\text{inv}} \in [1]_{\gamma^{\text{op}-1}}} \overline{t}v_{te,(\gamma^{\text{inv}},\gamma^{\text{op}})}^{\text{CH}_4\downarrow} \quad \forall \gamma^{\text{op}} \in \Gamma \setminus \{1\}, \quad (13b)$$

$$\overline{t}v_{te,(1,\gamma^{\text{op}})}^{\text{CH}_4\downarrow} \leq \overline{TV}_{te,0}^{\text{CH}_4} + \overline{t}v_{te,1}^{\text{CH}_4\uparrow} - \sum_{\bar{\gamma}^{\text{op}} \in [2]_{\gamma^{\text{op}-1}}} \overline{t}v_{te,(1,\bar{\gamma}^{\text{op}})}^{\text{CH}_4\downarrow} - \sum_{\bar{\gamma}^{\text{op}} = [1]_{\gamma^{\text{op}}}} \overline{t}v_{te,(1,\bar{\gamma}^{\text{op}})}^{\text{CH}_4,\text{rep}\downarrow} \quad \forall \gamma^{\text{op}} \in \Gamma \setminus \{1\}, \quad (13c)$$

$$\overline{t}v_{te,(\gamma^{\text{inv}},\gamma^{\text{op}})}^{\text{CH}_4\downarrow} \leq \overline{t}v_{te,\gamma^{\text{inv}}}^{\text{CH}_4\uparrow} - \sum_{\bar{\gamma}^{\text{op}} \in [\gamma^{\text{inv}}+1]_{\gamma^{\text{op}-1}}} \overline{t}v_{te,(\gamma^{\text{inv}},\bar{\gamma}^{\text{op}})}^{\text{CH}_4\downarrow} - \sum_{\bar{\gamma}^{\text{op}} = [\gamma^{\text{inv}}]_{\gamma^{\text{op}}}} \overline{t}v_{te,(\gamma^{\text{inv}},\bar{\gamma}^{\text{op}})}^{\text{CH}_4,\text{rep}\downarrow} \quad \forall (\gamma^{\text{inv}}, \gamma^{\text{op}}) \in \mathbb{N}^{\text{dec}}, \quad (13d)$$

where the parameter $\overline{TV}_{te,0}^{\text{CH}_4}$ corresponds to the initial capacity of LNG terminals. The LNG imports $ln_{g,t,\gamma}$ are limited by the import capacity of $\overline{t}v_{te,\gamma^{\text{op}}}^{\text{CH}_4}$. The corresponding constraint writes as follows $\forall te \in \mathcal{TE}^{\text{CH}_4}, \forall \gamma \in \Gamma$:

$$\sum_{t \in \mathcal{T}_\gamma} ln_{te,t,\gamma} \leq \overline{t}v_{te,\gamma^{\text{op}}}^{\text{CH}_4}. \quad (14)$$

Hydrogen (H₂) Decisions for the available H₂ terminal capacity $\overline{t}v_{te,\gamma^{\text{op}}}^{\text{H}_2}$ are explicitly modelled for every planning period, so that $\forall te \in \mathcal{TE}^{\text{H}_2}, \forall i \in \mathcal{I}$:

$$\overline{t}v_{te,1}^{\text{H}_2} = \overline{TV}_{te,0}^{\text{H}_2} + \overline{t}v_{te,1}^{\text{H}_2\uparrow} + \overline{t}v_{te,(1,1)}^{\text{H}_2,\text{rep}\uparrow}, \quad (15a)$$

$$\overline{t}v_{te,\gamma^{\text{op}}}^{\text{H}_2} = \overline{t}v_{te,\gamma^{\text{op}-1}}^{\text{H}_2} + \overline{t}v_{te,\gamma^{\text{op}}}^{\text{H}_2\uparrow} + \sum_{\gamma^{\text{inv}} \in [1]_{\gamma^{\text{op}}}} \overline{t}v_{te,(\gamma^{\text{inv}},\gamma^{\text{op}})}^{\text{H}_2,\text{rep}\uparrow} - \sum_{\gamma^{\text{inv}} \in [1]_{\gamma^{\text{op}-1}}} \overline{t}v_{te,(\gamma^{\text{inv}},\gamma^{\text{op}})}^{\text{H}_2\downarrow} \quad \forall \gamma^{\text{op}} \in \Gamma \setminus \{1\},$$

$$\overline{t}v_{te,(1,\gamma^{\text{op}})}^{\text{H}_2\downarrow} \leq \overline{TV}_{te,0}^{\text{H}_2} + \overline{t}v_{te,1}^{\text{H}_2\uparrow} - \sum_{\bar{\gamma}^{\text{op}} \in [2]_{\gamma^{\text{op}-1}}} \overline{t}v_{te,(1,\bar{\gamma}^{\text{op}})}^{\text{H}_2\downarrow} + \sum_{\bar{\gamma}^{\text{op}} = [1]_{\gamma^{\text{op}}}} \overline{t}v_{te,(1,\bar{\gamma}^{\text{op}})}^{\text{H}_2,\text{rep}\uparrow} \quad \forall \gamma^{\text{op}} \in \Gamma \setminus \{1\}, \quad (15b)$$

$$\overline{t}v_{te,(\gamma^{\text{inv}},\gamma^{\text{op}})}^{\text{H}_2\downarrow} \leq \overline{t}v_{te,\gamma^{\text{inv}}}^{\text{H}_2\uparrow} - \sum_{\bar{\gamma}^{\text{op}} \in [\gamma^{\text{inv}}+1]_{\gamma^{\text{op}-1}}} \overline{t}v_{te,(\gamma^{\text{inv}},\bar{\gamma}^{\text{op}})}^{\text{H}_2\downarrow} + \sum_{\bar{\gamma}^{\text{op}} = [\gamma^{\text{inv}}]_{\gamma^{\text{op}}}} \overline{t}v_{te,(\gamma^{\text{inv}},\bar{\gamma}^{\text{op}})}^{\text{H}_2,\text{rep}\uparrow} \quad \forall (\gamma^{\text{inv}}, \gamma^{\text{op}}) \in \mathbb{N}^{\text{dec}}, \quad (15c)$$

$$\overline{t}v_{te,(\gamma^{\text{inv}},\gamma^{\text{op}})}^{\text{H}_2,\text{rep}\uparrow} = \sum_{a' \in \delta^{\text{CH}_4}(a)} RF_a \overline{t}v_{a',(\gamma^{\text{inv}},\gamma^{\text{op}})}^{\text{CH}_4,\text{rep}\downarrow} \quad \forall \gamma^{\text{op}} \in \Gamma. \quad (15d)$$

The LH₂ imports $lh_{g,t,\gamma}$ are limited by the import capacity of a $\overline{t}v_{te,\gamma^{\text{op}}}^{\text{H}_2}$. The corresponding constraint writes as follows $\forall te \in TE^{\text{H}_2}, \forall \gamma \in \Gamma$:

$$\sum_{t \in \mathcal{T}_\gamma} lh_{te,t,\gamma} \leq \overline{t}v_{te,\gamma^{\text{op}}}^{\text{H}_2}. \quad (16)$$

2.4 Model improvement for market uptake and decommissioning restrictions

The model aims to optimise cost-efficiency by constructing H₂ and CH₄ infrastructure components as late as possible or repurposing and decommissioning them. The improvements address a more realistic system transformation behaviour by considering market growth constraints and avoiding unrealistic overnight build-outs while developing or dismantling gas infrastructure components.

2.4.1 Market growth rate restrictions

Scaling up projects that construct new or repurpose existing infrastructure components, i.e. pipeline and storage sites, are subject to many potential challenges and restrictions given an initial lack of market maturity. For instance, adopting and expanding new or reusing existing technologies may encounter high upfront costs with hesitant investment behaviour, compatibility and integration issues, regulatory and compliance hurdles, skill gaps, vendor lock-ins or bottlenecks.

To better understand and address those restrictions in the modelling framework, we introduce an annual market growth rate parameter $GR \in \mathbf{R}$, such that $GR > 1$, reflecting fast adoption or a slow-growing market environment in the transformation pathway. The parameter links the capacity expansion decisions of a given planning period with those of the previous planning period, and the corresponding capacity expansion and decommissioning constraints are written as follows $\forall a \in \mathcal{A}$:

$$\bar{p}_{a,\gamma^{inv}}^{H_2\uparrow} \leq \bar{p}_{a,\gamma^{inv-1}}^{H_2\uparrow} GR^{\Delta\gamma} \quad \forall \gamma^{inv} \in \Gamma \setminus \{1\}, \quad (17a)$$

$$\sum_{\gamma^{op} \in [1]_{\gamma^{inv}}} \bar{p}_{a,(\gamma^{inv},\gamma^{op})}^{H_2,rep\uparrow} \leq \sum_{\gamma^{op} \in [1]_{\gamma^{inv-1}}} GR^{\Delta\gamma} \bar{p}_{a,\gamma^{inv-1},\gamma^{op}}^{H_2,rep\uparrow} \quad \forall \gamma^{inv} \in \Gamma \setminus \{1\} \text{ such that } PR_{a,\gamma^{inv}} > 0. \quad (17b)$$

The parameter $PR_{a,\gamma^{inv}}$ restricts new construction and repurposing of each pipeline by means of a fixed and individual capacity limit for each period. As long as $PR_{a,\gamma^{inv}} = 0$, new construction and repurposing are completely prohibited. The restriction formulated above only begins as soon as these are permitted. Storages with the restriction parameter $SR_{a,\gamma^{inv}}$ are treated in the same way. Note that those parameters are node-specific, which could easily be applied to the entire system. Reasons for this are national differences in workforce and industry. Also note that the market growth rate only poses a restriction if the growth rate is small enough, e.g. over seven periods, an annual growth rate of 1.02 implies a doubling of capacity in the last period. Assuming a GR value of 1.25 would allow for more than 2000 times the initial capacity. Hence, if the growth rate is large enough, the constraints do not pose a restriction.

2.4.2 Decommissioning restrictions

Similarly, the decommissioning decisions of pipeline CH₄ facilities are restricted in the following manner $\forall a \in \mathcal{A}^{CH_4}$ and $\forall (\gamma^{inv}, \gamma^{op}) \in \leq^{\text{dec}} : \gamma^{inv} > \gamma^{inv,\text{min}}$:

$$\sum_{\bar{\gamma}^{inv} \in [1]_{\gamma^{op-1}}} \bar{p}_{a,(\bar{\gamma}^{inv},\gamma^{op})}^{CH_4\downarrow} \leq \sum_{\bar{\gamma}^{inv} \in [1]_{\gamma^{op-2}}} GR^{\Delta\gamma} \bar{p}_{a,(\bar{\gamma}^{inv},\gamma^{op-1})}^{CH_4\downarrow}. \quad (18)$$

The same approach holds for storage $\forall s \in \mathcal{S}^{CH_4}$ and $\forall (\gamma^{inv}, \gamma^{op}) \in \leq^{\text{dec}} : \gamma^{inv} > \gamma^{inv,\text{min}}$:

$$\sum_{\bar{\gamma}^{inv} \in [1]_{\gamma^{op-1}}} \bar{sv}_{s,(\bar{\gamma}^{inv},\gamma^{op})}^{CH_4\downarrow} \leq \sum_{\bar{\gamma}^{inv} \in [1]_{\gamma^{op-2}}} GR^{\Delta\gamma} \bar{sv}_{s,(\bar{\gamma}^{inv},\gamma^{op-1})}^{CH_4\downarrow}. \quad (19)$$

The same approach holds for terminals $\forall te \in \mathcal{T}^{\mathcal{E}^{CH_4}}$ and $\forall (\gamma^{inv}, \gamma^{op}) \in \leq^{\text{dec}} : \gamma^{inv} > \gamma^{inv,\text{min}}$:

$$\sum_{\bar{\gamma}^{inv} \in [1]_{\gamma^{op-1}}} \bar{tv}_{s,(\bar{\gamma}^{inv},\gamma^{op})}^{CH_4\downarrow} \leq \sum_{\bar{\gamma}^{inv} \in [1]_{\gamma^{op-2}}} GR^{\Delta\gamma} \bar{tv}_{s,(\bar{\gamma}^{inv},\gamma^{op-1})}^{CH_4\downarrow}. \quad (20)$$

2.5 Objective and optimisation problem

The model minimises total costs for investment f^{inv} and system operation f^{op} decisions for all planning periods, covering pipeline, storage and terminal investments as well as operational costs for fuel production and conversion, see Equation (21a). The investment costs in Equation (21b) consist of the new installation costs f^{new} defined in Equation (21c), the repurposing costs f^{rep} defined in Equation (21d), and the decommissioning costs (including lifetime compensation payments) f^{dec} defined in Equation (21e). The objective function f of the underlying LP is:

$$\min_{(p,sv,tv,ng,bh,ln,lh,gh,gy) \in \mathcal{D}} f = f^{inv} + f^{op}, \quad (21a)$$

s.t. Equations (1) to (20)

where $(p, sv, tv, ng, bh, ln, lh, gh, gy)$ is the tuple of all decision variables and \mathcal{D} its polyhedral feasible set defined by all system-wide and technology-dependent unit constraints formulated above. The objective function components for investment decisions are defined as

$$f^{inv} = f^{new} + f^{rep} - f^{dec}, \quad (21b)$$

$$f^{new} = \sum_{\gamma \in \Gamma} \left[\sum_{a \in \mathcal{A}^{CH_4}} C_{a,\gamma}^{inv} \overline{p}_{a,\gamma}^{CH_4 \uparrow} + \sum_{a \in \mathcal{A}^{H_2}} C_{a,\gamma}^{inv} \overline{p}_{a,\gamma}^{H_2 \uparrow} + \sum_{s \in \mathcal{S}^{CH_4}} C_{s,\gamma}^{inv} \overline{sv}_{s,\gamma}^{CH_4 \uparrow} + \sum_{s \in \mathcal{S}^{H_2}} C_{s,\gamma}^{inv} \overline{sv}_{s,\gamma}^{H_2 \uparrow} + \sum_{te \in \mathcal{T} \mathcal{E}^{CH_4}} C_{te,\gamma}^{inv} \overline{tv}_{te,\gamma}^{CH_4 \uparrow} + \sum_{te \in \mathcal{T} \mathcal{E}^{H_2}} C_{te,\gamma}^{inv} \overline{tv}_{te,\gamma}^{H_2 \uparrow} \right], \quad (21c)$$

$$f^{rep} = \sum_{\gamma \in \mathbb{F}^{rep}} \left[\sum_{a \in \mathcal{A}^{H_2}} C_{a,\gamma}^{rep} \overline{p}_{a,\gamma}^{H_2 \uparrow} + \sum_{s \in \mathcal{S}^{H_2}} C_{s,\gamma}^{rep} \overline{sv}_{s,\gamma}^{H_2 \uparrow} + \sum_{te \in \mathcal{T} \mathcal{E}^{H_2}} C_{te,\gamma}^{rep} \overline{tv}_{te,\gamma}^{H_2 \uparrow} \right], \quad (21d)$$

$$f^{dec} = \sum_{\gamma \in \mathbb{F}^{dec}} \left[\sum_{a \in \mathcal{A}^{CH_4}} C_{a,\gamma}^{dec} \overline{p}_{a,\gamma}^{CH_4 \downarrow} + \sum_{a \in \mathcal{A}^{H_2}} C_{a,\gamma}^{dec} \overline{p}_{a,\gamma}^{H_2 \downarrow} + \sum_{s \in \mathcal{S}^{CH_4}} C_{s,\gamma}^{dec} \overline{sv}_{s,\gamma}^{CH_4 \downarrow} + \sum_{s \in \mathcal{S}^{H_2}} C_{s,\gamma}^{dec} \overline{sv}_{s,\gamma}^{H_2 \downarrow} + \sum_{te \in \mathcal{T} \mathcal{E}^{CH_4}} C_{te,\gamma}^{dec} \overline{tv}_{te,\gamma}^{CH_4 \downarrow} + \sum_{te \in \mathcal{T} \mathcal{E}^{H_2}} C_{te,\gamma}^{dec} \overline{tv}_{te,\gamma}^{H_2 \downarrow} \right], \quad (21e)$$

where the parameter $C_{(\cdot),\gamma}^{inv}$ captures the fixed operation costs and the corresponding specific lifetime investment costs for new capacity investments. Note that these entail lifetime investment and reinvestment costs with a perpetuity approach after the explicitly modelled planning periods. $C_{(\cdot),\gamma}^{rep}$ captures the fixed operation costs and the corresponding specific lifetime investment costs for repurposing capacity investments. $C_{(\cdot),\gamma}^{dec}$ captures the specific decommissioning costs and compensation payments matching the avoided fixed operation costs and specific lifetime investment for decommissioning of capacity. Figure 2 illustrates the complex multi-period capacity and investment relations discussed above. It shows the capacity decisions and costs for three investment streams in a three-period capacity expansion planning instance of the IMAGINE model. The approach offers several advantages when capturing new expansion,

		Operational period (γ^{op})										
		1			2			3				
Investment period (γ^{inv})	1	Available	$\overline{p}_{a,(1,1)}^{H_2}$		Available	$\overline{p}_{a,(1,2)}^{H_2}$		Available	$\overline{p}_{a,(1,3)}^{H_2}$		Investment stream 1	
		Expansion	$\overline{p}_{a,(1)}^{H_2 \uparrow}$	$C_{a,1}^{inv}$	Repurposing	$\overline{p}_{a,(1,2)}^{H_2,rep \uparrow}$	$C_{a,2}^{rep}$	Repurposing	$\overline{p}_{a,(1,3)}^{H_2,rep \uparrow}$	$C_{a,3}^{rep}$		
		Repurposing	$\overline{p}_{a,(1,2)}^{H_2,rep \uparrow}$	$C_{a,1}^{rep}$	Decommissioning	$\overline{p}_{a,(1,2)}^{H_2 \downarrow}$	$C_{a,2}^{dec}$	Decommissioning	$\overline{p}_{a,(1,3)}^{H_2 \downarrow}$	$C_{a,3}^{dec}$		
	2				Available	$\overline{p}_{a,(2,2)}^{H_2}$		Available	$\overline{p}_{a,(2,3)}^{H_2}$			Investment stream 2
		Expansion	$\overline{p}_{a,(2)}^{H_2 \uparrow}$	$C_{a,2}^{inv}$	Repurposing	$\overline{p}_{a,(2,3)}^{H_2,rep \uparrow}$	$C_{a,3}^{rep}$	Repurposing	$\overline{p}_{a,(2,3)}^{H_2,rep \uparrow}$	$C_{a,3}^{rep}$		
		Repurposing	$\overline{p}_{a,(2,2)}^{H_2,rep \uparrow}$	$C_{a,2}^{rep}$	Decommissioning	$\overline{p}_{a,(2,3)}^{H_2 \downarrow}$	$C_{a,3}^{dec}$	Decommissioning	$\overline{p}_{a,(2,3)}^{H_2 \downarrow}$	$C_{a,3}^{dec}$		
	3							Available	$\overline{p}_{a,(3,3)}^{H_2}$			Investment stream 3
		Expansion	$\overline{p}_{a,(3)}^{H_2 \uparrow}$	$C_{a,3}^{inv}$	Expansion	$\overline{p}_{a,(3)}^{H_2 \uparrow}$	$C_{a,3}^{inv}$	Expansion	$\overline{p}_{a,(3)}^{H_2 \uparrow}$	$C_{a,3}^{inv}$		
		Repurposing	$\overline{p}_{a,(3,3)}^{H_2,rep \uparrow}$	$C_{a,3}^{rep}$	Repurposing	$\overline{p}_{a,(3,3)}^{H_2,rep \uparrow}$	$C_{a,3}^{rep}$	Repurposing	$\overline{p}_{a,(3,3)}^{H_2,rep \uparrow}$	$C_{a,3}^{rep}$		

Figure 2: Endogenous capacity decisions and corresponding cost parameters for three investment streams in the multi-period capacity expansion planning model IMAGINE, own illustration.

decommissioning, and refurbishment decisions in a path-dependent system transition. Firstly, it provides a detailed overview of all investment streams, allowing for in-depth analysis of capacity changes, new build-outs, and decommissioning. Additionally, it enables consideration of technological improvements in future investment periods, such as enhancements in availability profiles or efficiency of specific technologies. Moreover, the method allows for more detailed analysis of repurposing existing or yet-to-be-built capacity.

The objective function components for system operation decisions in every considered time step $t \in T$ are defined as

$$\begin{aligned}
f^{\text{op}} = & \sum_{\gamma \in \Gamma} \left[\sum_{t \in \mathcal{T}_\gamma} \left(\sum_{g \in \mathcal{NG}} C_{g,\gamma}^{\text{op}} n g_{g,t,\gamma} + \sum_{g \in \mathcal{B}h} C_{g,\gamma}^{\text{op}} b h_{g,t,\gamma} + \sum_{g \in \mathcal{G}H} C_{g,\gamma}^{\text{op}} g h_{g,t,\gamma} + \sum_{g \in \mathcal{S}NG} C_{g,\gamma}^{\text{op}} s n_{g,t,\gamma} \right. \right. \\
& + \sum_{g \in \mathcal{G}Y} C_{g,\gamma}^{\text{op}} g y_{g,t,\gamma} + \sum_{a \in \mathcal{A}^{\text{CH}_4}} C_{a,\gamma}^{\text{op}} p_{a,t,\gamma}^{\text{CH}_4} + \sum_{a \in \mathcal{A}^{\text{H}_2}} C_{a,\gamma}^{\text{op}} \left(p_{(i,j),t,\gamma}^{\text{H}_2} + p_{(j,i),t,\gamma}^{\text{H}_2} \right) + \sum_{s \in \mathcal{S}^{\text{CH}_4}} C_{s,\gamma}^{\text{op}} \\
& \left. \left(p_{s,t,\gamma}^{\text{CH}_4,\text{wd}} + p_{s,t,\gamma}^{\text{CH}_4,\text{in}} \right) + \sum_{s \in \mathcal{S}^{\text{H}_2}} C_{s,\gamma}^{\text{op}} \left(p_{s,t,\gamma}^{\text{H}_2,\text{wd}} + p_{s,t,\gamma}^{\text{H}_2,\text{in}} \right) + \sum_{te \in \mathcal{T}\mathcal{E}^{\text{CH}_4}} C_{te,\gamma}^{\text{op}} l n_{te,t,\gamma} + \sum_{te \in \mathcal{T}\mathcal{E}^{\text{H}_2}} C_{te,\gamma}^{\text{op}} l h_{te,t,\gamma} \right) \Big]. \quad (21f)
\end{aligned}$$

where $C_{(\cdot),\gamma}^{\text{op}}$ are the operation costs for the corresponding dispatch decision variables for generation and consumption technologies.

3 Hydrogen storage sensitivity analysis

The case study consists of two steps (see Figure 1). First, SCOPE SD generates medium- and long-term scenarios for the future net-zero European energy system across seven expansion planning periods from 2020 to 2050 in five-year intervals, i.e. $\Gamma = \{1, \dots, 7\}$. Second, the SCOPE SD results provide input for IMAGINE to examine ten scenario variants that represent the uncertainty of H₂ storage costs and market uptake restrictions in the transformation pathways.

3.1 Structural and time series input data

Detailed information on input data and assumptions for the SCOPE SD instances can be found in recent publications, see [13, 14, 15, 16]. The case study setup uses the historical meteorological year 2012 (including its ‘‘Kalte Dunkelflaute’’ period) and assumes that Europe is climate-neutral by 2050. The scenario is based on [21] and visualised at Fraunhofer IEE’s *Transformationsatlas der Energiewende* [22] (Ariadne Base Scenario).

Running the IMAGINE modelling and optimisation framework requires additional structural and time series input data. Information on already existing pipelines in 2020 is taken from [23] and data on already existing storage capacities in 2020 is taken from [24] and for LNG terminals from [25]. Investment and operation costs for future pipelines are based on [7], for terminals on [26] and for storage on [27] and [28], see Table 2 in the appendix. As available cost information for decommissioning infrastructure is very limited in the literature, the case study approximates these at 10% of the corresponding investment costs [29]. The future underground H₂ storage potential including depleted hydrocarbon reservoirs and salt caverns is gathered from [8], which indicates a large but unevenly distributed technical potential of salt caverns across Europe.

Price and quantity assumptions for non-European export countries for renewable energy carriers are based on Fraunhofer IEE’s *Power-to-X atlas* [30]. Historical data for natural gas generation and gas reserves is taken from [31, 32]. LNG import costs are estimated using [33] and natural gas production costs are determined using [34].

Time series data of production and consumption as well as demand for H₂ and CH₄ are derived from the upstream SCOPE SD results. To that end, hourly results from SCOPE SD are aggregated to daily input data for the IMAGINE framework. The carbon price path is interpolated between a price of 50 EUR/tCO₂ in 2020 [35] and 400 EUR/tCO₂ by 2050, which is an endogenous result of the SCOPE SD model.

Note that all investment decisions are based on an interest rate of 6% and a depreciation of 50 years for pipelines and 50 years for storage. A social discount rate of 3% is assumed to consider the time value of money when making multi-period investment and decommissioning decisions in the IMAGINE framework.

3.2 Scenario setup

Experience with the construction and use of H₂ storage facilities is still limited. Due to the inherent individuality of each project and the ongoing technology development, it is difficult to forecast the exact costs and market uptake rates of deploying solutions involving this technology. To better understand the relationship between H₂ storage costs and market uptake rates for potential gas market and infrastructure transformation pathways, we perform a sensitivity analysis based on those two parameters.

Storage cost sensitivity Given the current uncertainty associated with H₂ storage investment costs, we explore a wide range of capital expenditure (CAPEX) projections based on very high and low estimates from the recent literature. More specifically, we assume the following two storage cost scenarios for newly-built H₂ storage facilities:

- *Low*: 269,393 EUR/GWh_{th} (BDI) [27],
- *High*: 1,500,000 EUR/GWh_{th} (DEA) [28],

and add eight intermediate cost steps in between for a storage cost range with a total of 10 variations (see Table 2 in the Appendix for detailed information). Note that the *Medium* storage cost scenario assumes 808,179 EUR/GWh_{th}. The cost variations apply to CAPEX, fixed operational expenditures (OPEX), and decommissioning costs. The variable OPEX are not part of the variation as they are not expected to change proportionally with the other economic parameters.

Market growth rate sensitivity In a second part, we conduct a sensitivity analysis varying the market growth rate parameters, see Section 2.4.1. We analyse the following four different growth rate restrictions:

- $GR = 1.05$,
- $GR = 1.25$,
- $GR = 1.50$,
- $GR = \infty$ (no restriction).

While the storage cost sensitivity analysis assumes a constant $GR = 1.25$ for the storage cost range, the market growth rate sensitivity analysis also takes storage cost variations into account, i.e. *Low*, *Medium*, and *High*. In total, both sensitivity analyses result in 19 individual IMAGINE model runs.

Simulation setup As mentioned, the IMAGINE framework is formulated as a LP optimisation model, and the resulting large-scale LP instances are solved with the Barrier (interior point) algorithm of Gurobi Optimizer Version 11.0 [36] on a medium-range HPCC node at Fraunhofer IEE (Intel XEON E5-2698v3 16 Cores@2.30 GHz, 256 GB). The matrix size is characterised as follows: 9.2 million variables, 9.2 million constraints and 38 million non-zero entries. Solving times of the problem instances vary between 45 min and one hour.

4 Results and discussion

In this section, we analyse the scenario results based on our model. Our aim is to explore how the uncertainty of costs for H₂ storage and market uptake restrictions impacts the transition in Europe and the long-term H₂ economy. We present the results in two parts: Section 4.1 shows the overall infrastructure deployments and infrastructure operation in the transformed (finale state) system, and Sections 4.2 to 4.4 illustrates the results of the parameter variations and the system transformation pathways.

4.1 Transformed system

Infrastructure demands in the transformed system Figure 3 illustrates the installed capacities of H₂ storage and pipelines across Europe. Different H₂ storage costs significantly affect the gas infrastructure development until 2050. Europe’s H₂ storage development concentrates on the salt cavern potential in central Europe, particularly in the market areas of Germany, Poland, France, Netherlands, and Great Britain. In the low-cost scenario, we observe substantial installations of new H₂ storage. Moreover, the results show that, except for the high storage cost scenario, the potential of repurposing CH₄ storage is largely exploited. At the same time, there are only limited installations of new H₂ storage systems.

Great Britain’s continuing natural gas consumption creates challenges in repurposing CH₄ storage as the market growth rate imposes restrictions. The initial repurposing decisions would have to start at an earlier stage, which is impossible due to the continuing CH₄ consumption. With increasing storage costs, the model compensates for repurposed natural gas storage with pipelines. Hence, Great Britain is an outlier in the repurposing of storage facilities and seems to be build out exactly the same amount of storage in all scenarios.

In contrast, Germany experiences the most significant decrease in storage build-out as storage costs increase. More than the half of the less installed storage across Europe in 2050 between the low- and high-cost scenario comes from Germany. This highlights Germany’s role as a central transit country in Europe. Additional pipeline investments may

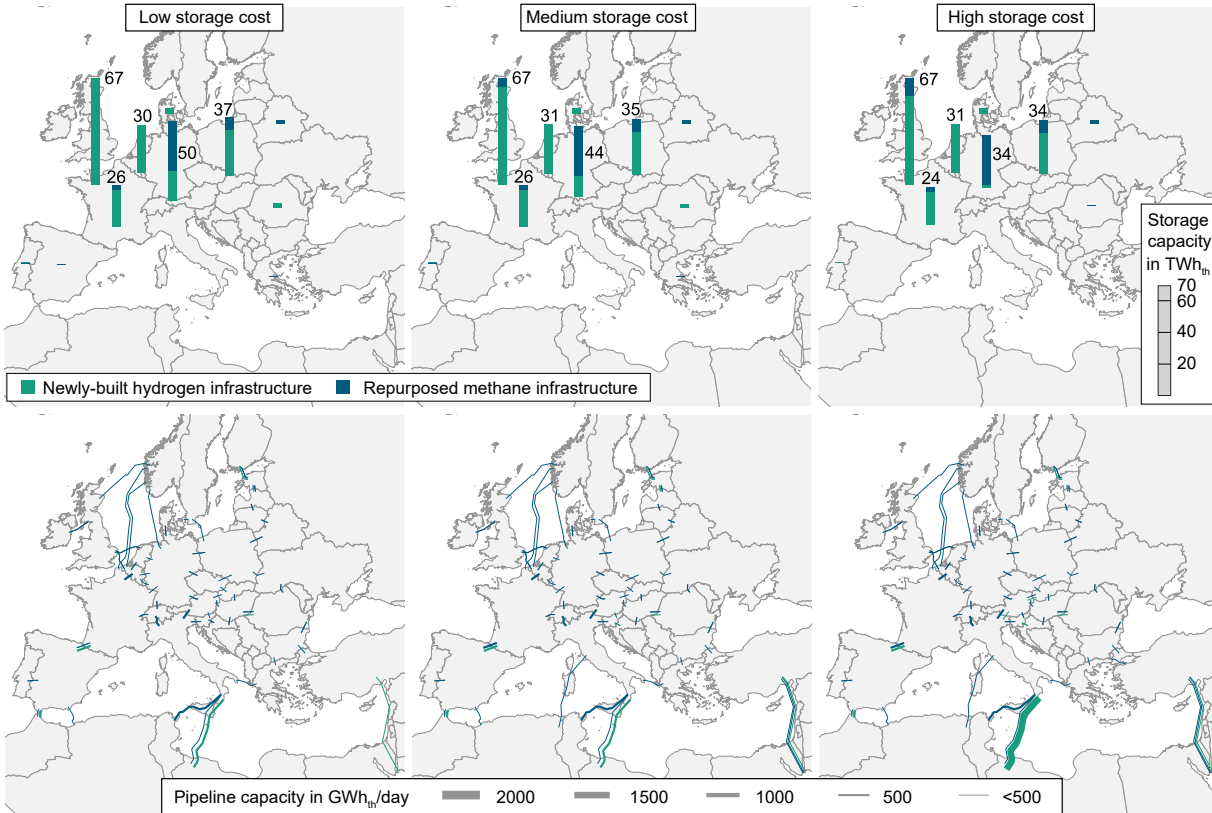


Figure 3: Installed capacities of H₂ storage (top) and pipelines (bottom) across Europe for the low, medium, and high storage cost scenarios in the transformed system by 2050 ($GR = 1.25$), own illustration based on optimisation results.

compensate for the lack of storage infrastructure in Germany. However, this may not be the case for other countries that are less connected in the European H₂ network due to their geographical location. Considering no network restrictions within a node like Germany also impacts the results for storage needs.

As expected, pipeline developments have opposite effects. In the low-cost scenario, the largest capacity consists of repurposed pipeline capacity. In the high-cost scenario, new H₂ pipeline capacity is installed to connect the Middle East and North Africa (MENA) region with Central Europe. This is particularly evident for the pipeline links from Libya to Italy. The H₂ import capacity grows by 1 TWh_{th}/day, while the pipeline capacity from the other European countries to Italy grows by 0.5 TWh_{th}/day. For example, this connection can compensate for reduced storage build-outs in Central Europe for the high-cost scenario.

Infrastructure operation in the transformed system A comparison of the daily dispatch results for the entire year of 2050 in the low- and high storage cost scenarios shows that seasonal demand variations are met by either significant storage expansion or more extensive pipeline infrastructure within Europe and from the exporting MENA region to Europe, see Figure 4).

Note that all storage systems' initial and final volume levels are linked by an inequality constraint, which requires the final volume level to be greater than or equal to the initial volume level. Therefore, the observed storage trajectories, including the initial and final volume levels, are endogenous decisions optimised by the model.

As mentioned in the Section 3.1, 2012 was chosen as the meteorological input year and the effect of the “Kalte Dunkelflaute” is highlighted in Figure 4. During the two weeks, it is evident that the energy system suffers from a lack of renewable electricity generation and heat supply coinciding with high energy consumption during cold winter days. The European energy system and its security of supply depend on the energy carrier H₂ during that period. On the one hand, H₂ storage investments depend on the assumed costs. On the other hand, working gas injection and withdrawal ratios play a crucial role in the expansion decisions. These are also uncertain parameters due to limited knowledge of existing and future storage configurations. Table 1 presents the difference between installed capacity, the so-called working gas volume, and the actually used storage volume. Note that the maximum used volume must

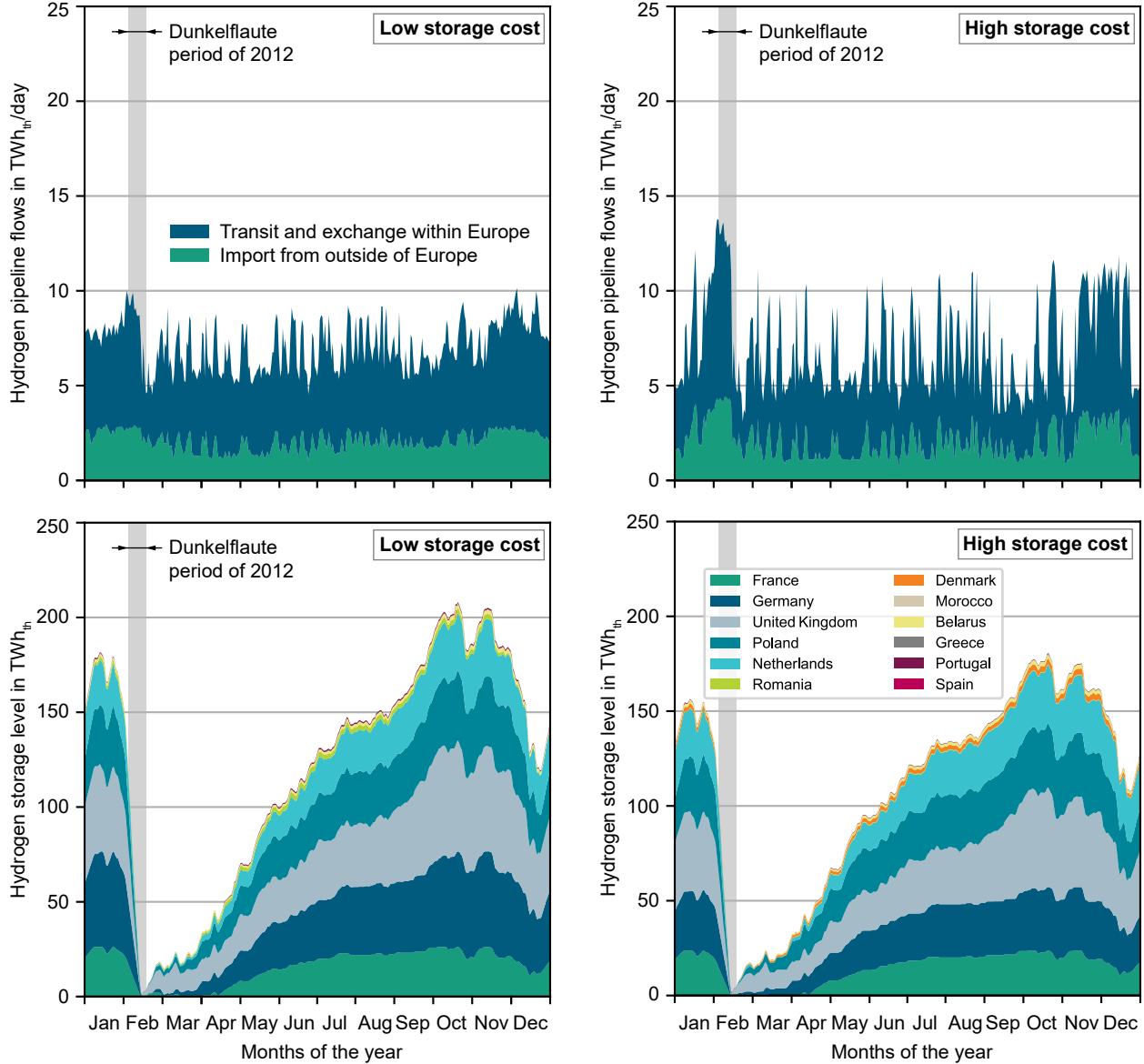


Figure 4: H₂ pipeline flows (top) and H₂ storage (salt cavern) trajectory (bottom) for the low (left) and high (right) storage cost scenarios assuming a market growth rate of $GR = 1.25$, own illustration based on optimisation results.

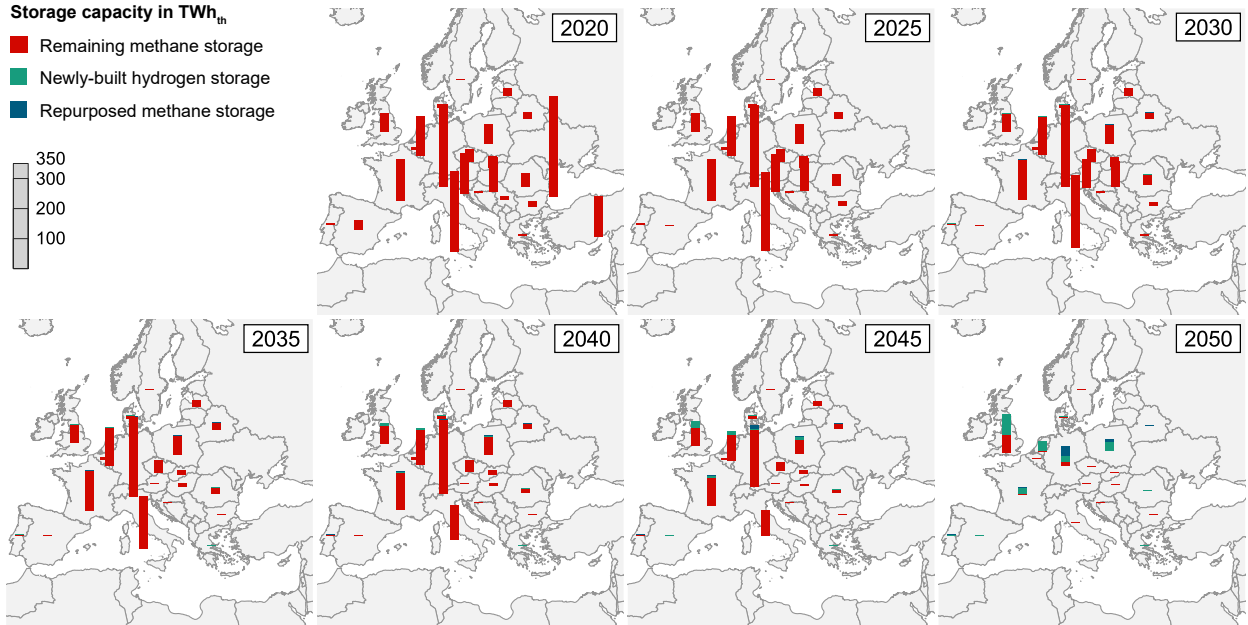
be lower than the installed capacity. The data of existing gas storage facilities are heterogeneous in their technical specification. While depleted fields or aquifers feature higher working gas to injection or withdrawal design ratios of over $70 \text{ GWh}_{\text{th}}/\text{GW}_{\text{th}}$, salt caverns feature around 30 to $50 \text{ GWh}_{\text{th}}/\text{GW}_{\text{th}}$ (weighted mean), see [24]. Different assumptions for those parameters significantly influence the installed capacity results. The results of the mean design ratio for the combination of new build and repurposed storage are given in Table 1.

4.2 Transformation pathways

All scenario variants include path-dependent investment and decommissioning decisions. Figure 5 illustrates the path-dependent development of H₂ storage in Europe for the low storage cost scenario with a market growth rate of 1.25. A key result is the late (2045-2050) build-out of storage facilities in Europe, which results from the seasonal demand patterns in the long-term system states with achieved carbon neutrality. In the medium-term planning periods, i.e. 2030-2045, the less seasonal H₂ demand is met by H₂ exchange via pipelines. Note that, due to the use of renewable

Table 1: Hydrogen (H_2) storage and pipeline capacity relation of installed capacity and used capacity in 2050 ($\gamma^{op} = 7$).

Storage cost scenario (2050)	Low	High
Share of repurposed storage in %	20.2	28.8
Installed capacity $\sum_{s \in S^{H_2}} \bar{s}v_{s,7}^{H_2}$ in TWh_{H_2}	220.6	195.2
$\max_{t \in T_7} (\sum_{s \in S^{H_2}} sl_s(t))$ in TWh_{H_2}	212.0	180.6
Share of repurposed pipelines in %	77.5	82.9
Installed capacity $\sum_{a \in A^{H_2}} \bar{p}_{a,7}^{H_2}$ in TWh_{H_2}/d	12.5	15.4
$\max_{t \in T_7} (\sum_{a \in A^{H_2}} p_a^{H_2})$ in TWh_{H_2}/d	10.1	13.8

Figure 5: Hydrogen (H_2) storage expansion pathway for all considered market areas at the low-cost scenario and a market growth rate of $GR = 1.25$, own illustration based on optimisation results.

electricity and more efficient technologies, e.g. heat pumps, the demands for H_2 and, ultimately, H_2 storage are smaller compared to today's CH_4 storage needs.

Great Britain stands out with its continued higher storage demand for CH_4 . Possible reasons include the island location, decommissioning constraints enforced by the market growth rate, and a distinct CH_4 consumption pattern including a considerable share of gas-based thermal power plants. Note that some of arguments also apply to Germany which has a comparatively smaller but still visible sustained demand for CH_4 storage.

4.3 Impacts of hydrogen storage cost

Capacity investments The total investment decisions in H_2 storage and pipeline capacity for all ten cost scenarios can be observed in Figure 6. Except for United Kingdom, the storage repurposing potentials are fully exploited in the scenarios with additional market uptake restrictions. For pipelines, the capacity generally increases slightly, as indicated by the green bars. The share of repurposing capacity for storage ranges from 20.2% in the low storage cost scenario to 28.8% in the high storage cost scenario. The share of repurposed pipeline assets varies from 82.9% to 77.5%. The installed H_2 storage capacity ranges from 220.6 TWh_{th} to 195.2 TWh_{th} , and the transport capacity via pipelines ranges from 12.5 TWh_{th}/d to 15.4 TWh_{th}/d .

Lifetime costs analysis Because the objective function of the optimisation minimises the total lifetime costs, the resulting investment and operation costs are essential results. The investment costs capture those for capacity expansion or

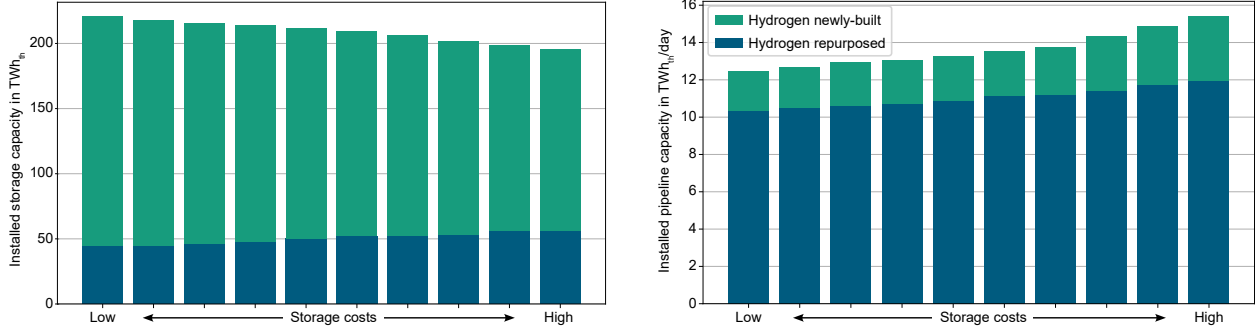


Figure 6: Pan-European storage (top) and pipeline (bottom) capacity expansion results for the considered range of uncertain storage cost parameters ($GR = 1.25$), own illustration based on optimisation results.

repurposing decisions, and decommissioning costs (including lifetime compensation payments) for decommissioned infrastructure. The costs can also be separated into period-specific and lifetime investment costs, which are the sum over the entire multi-period planning horizon until the final state of the system is reached. Varying only one parameter in the optimisation, e.g. the storage investment costs, largely affects the solution and composition of the H_2 and CH_4 infrastructure, see Figure 7. In the high-cost scenario, the overall system costs increase by around 6.2% compared to the low storage cost scenario.

As more H_2 pipeline infrastructure is needed earlier in the transformation pathways, there is an extended need for LNG in the markets, see Figure 7. The largest share of the lifetime costs is incurred by natural gas imports and the H_2 produced outside of Europe, see the left plot in Figure 7.

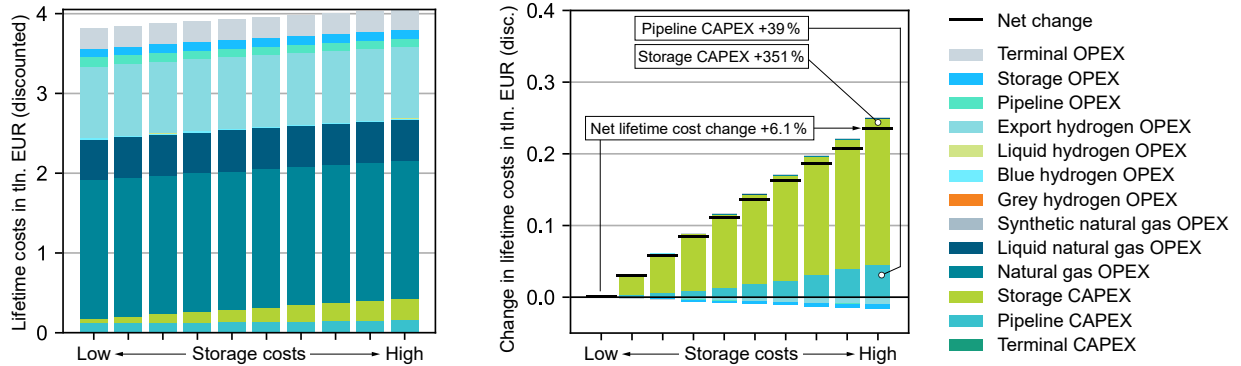


Figure 7: Comparison of resulting total and change in lifetime discounted costs for the considered low to high H_2 storage cost scenarios and the market growth rate variant $GR = 1.25$, own illustration based on optimisation results.

4.4 Impacts of market growth restrictions

The model results demonstrate that the market growth rate plays a crucial role in determining the expansion of H_2 storage, as well as the repurposing and decommissioning of CH_4 storage facilities, as shown in Figure 8. Due to the continued consumption of CH_4 in the later periods, a strong shift in the trajectory is not feasible given stricter market growth rates. The findings indicate that the market growth rate has a substantial influence on optimising infrastructure investments and prevents abrupt build-outs.

Figure 9 illustrates the coactive effects of varying market growth rate restrictions and storage investment costs for on H_2 storage demands in Europe and Germany. Note that the individual results for capacity expansion and refurbishing are given in Figures 11 and 12, respectively. Comparing the results between Europe (left) and Germany (right) in Figure 9, it is evident that the storage demand in Germany is strongly affected by the storage cost sensitivities, while the European total H_2 storage demands show smaller variations. Between 2030 and 2045, the assumed growth rate determines how early the new and refurbishing investments need to pick up in order to meet the long-term H_2 demands. Without market growth rate restrictions, H_2 storage demands will begin to emerge by 2035 or 2040. However, if market growth restrictions are imposed, the modelling results exhibit storage build-outs between 2025 and 2030. The growth

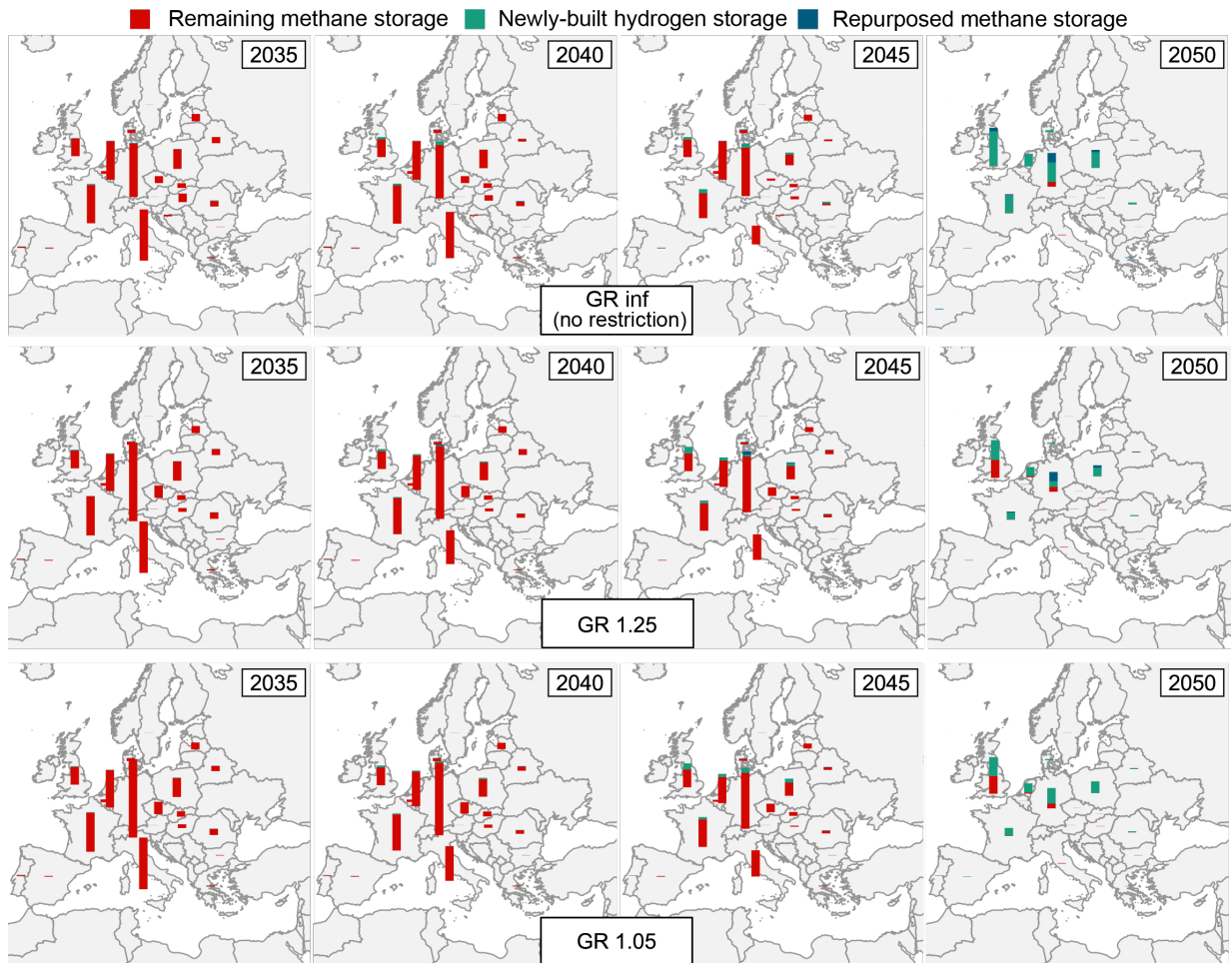


Figure 8: Impacts of different market growth rates (infinity, 1.25, 1.05) on installed H₂ storage capacity in Europe from 2035 to 2050 for the low-cost storage cost scenario, own illustration based on optimisation results.

rate restrictions mostly affect the path-dependent investment trajectories, whereas the storage costs have the greatest impact on the final H₂ storage demand by 2050.

The gap between 2045 and 2050 is large for all variants except for the 1.05 growth rate variants. Even in the 1.25 variants, the installed capacity for hydrogen storage in Europe tripled in these five years. The difference between 2045 and 2050 is even higher in the low-cost scenarios. To assume realistic market growth, a growth rate lower than 1.25 should be considered.

Figure 10 in the appendix shows Europe’s resulting aggregated H₂ pipeline capacities, comparing the pipeline investment decisions for different H₂ storage costs and market growth rates. It is clear that the impact of the growth rates is much lower for pipelines than for storage, which may be due to the need for more exchange capacity within Europe in earlier years, as well as to more repurposing and fewer construction projects for new pipelines.

4.5 Discussion

4.5.1 Summary and reflection

The case study results demonstrate the possibility of integrating H₂ as a key piece into a climate-neutral energy system. As other studies focus on the final configuration [6, 1, 5, 37], the IMAGINE modelling framework also incorporates the path-dependent decisions involved in the CH₄ and H₂ gas infrastructure development over multiple planning periods. Besides showing the interactions between different components of the gas infrastructure transformation, the approach allows us to shed light on two important uncertainties, i.e. H₂ storage costs and market uptake restrictions. The findings reveal significant influences on the demand trajectories for hydrogen storage. While the costs associated with

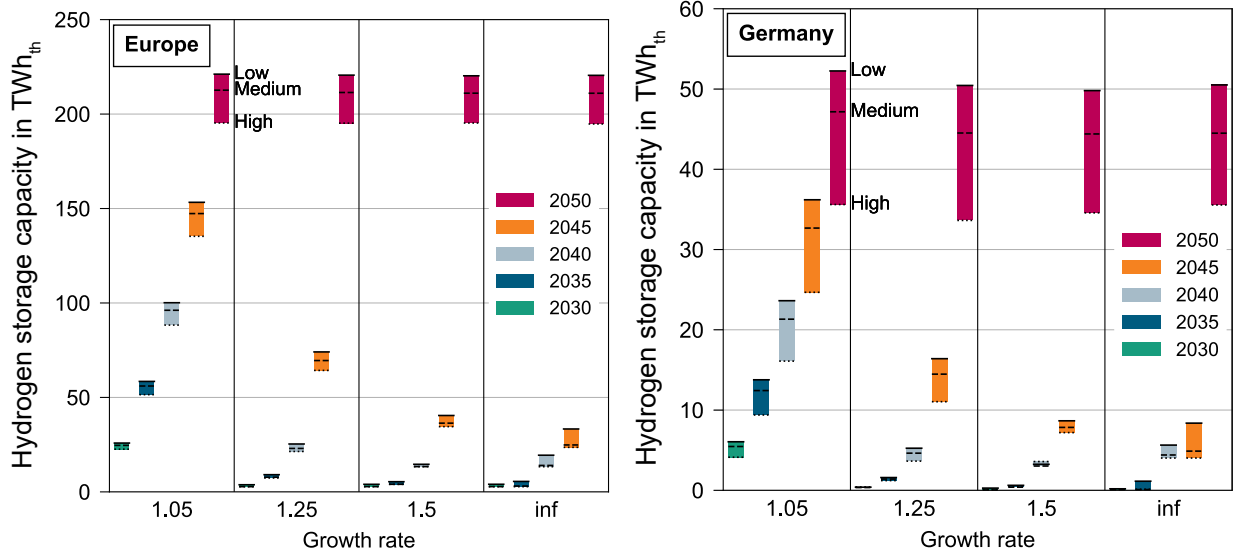


Figure 9: Total hydrogen (H_2) storage demand results (including expansion, refurbishing, and decommissioning) for four market growth rate variations (1.05, 1.25, 1.5, and infinity) and three storage cost scenarios (Low, Medium, High) in Europe (left) and Germany (right), own illustration based on optimisation results.

hydrogen storage predominantly determine the final gas infrastructure configuration of a net-neutral energy system, restrictions on market uptake critically affect the intermediate hydrogen storage demands across Europe. Additionally, the repurposing of natural gas infrastructure is crucial in all examined scenarios and nearly every country.

The soft-linking approach of the SCOPE SD and IMAGINE models results in a more inefficient system than integrating all decisions in one model because investment and operation decisions in electricity capacities and infrastructure are made without consideration of the gas infrastructure and market. However, due to varying technological readiness and policy environments, it is unknown whether full integration of all markets, including power, gas, and others, will eventually occur or remain elusive. Hence, our soft-linking approach might represent a pragmatic alignment with real-world market and infrastructure development processes.

Based on the scenario setup, we show that H_2 storage investments start as early as 2030 but become essential between 2045 and 2050, confirming the results in [12]. H_2 pipeline investments start in 2025 and ramp up until 2050. These results align with the work presented in [38], where the H_2 networks appear after 2035. Because of the extreme H_2 storage investments in 2045 and 2050, the model was extended to investigate the uncertainty associated with market uptake restrictions. As evidenced by Great Britain's case, the market growth rate plays a critical role in repurposing and decommissioning gas infrastructure components. The assumptions for the market growth rate exhibit substantial impacts, highlighting its relevance for multi-period expansion planning and the need for a better understanding and quantification of the market uptake processes and their restrictions. A market growth rate restriction, which in our case study means lower than 1.25, should be used to represent technology deployment and transformation pathways more realistically in the models. In addition to the uptake of the H_2 economy, individual storage and pipeline projects take time to build. For example, in [39], it is assumed that the construction of a new underground H_2 storage facility takes 15 years, and the repurposing takes up to five years.

Due to the key role of the MENA region, as well as the transit countries, the responsibility of building Europe's future H_2 network including environmental, social, and financial concerns need to be addressed in the pursuit of a just transition, e.g., see [40].

In the study conducted in [5], European climate neutrality scenarios were examined, considering electricity and H_2 network trade-offs along with integrated electricity and H_2 markets. The authors find cost-optimal H_2 storage demands in Europe of up to 43 TWh_{th}. By contrast, in [41], the demand for H_2 storage in Europe ranges between 143 and 268 TWh_{th}. In [8], the demand for H_2 storage is about 130 TWh_{th}. Our scenarios involve H_2 storage investments ranging from 195 to 220 TWh_{th} until 2050. There are a few important aspects to keep in mind when comparing the results with [5], which does not consider (green) H_2 imports from outside of Europe, implying that all H_2 (or derived fuels) will be produced within the European energy system. While the overall H_2 consumption in the final

planning period is at similar levels for all studies, the results obtained by our case study assume domestic electrolyser deployments of up to 410 GW_{el} as compared to 1250 GW_{el} in [5].

Moreover, when considering the possibility of importing renewable (storable) fuels into Europe, several factors influence gas storage demands in Europe. Weather-dependent export patterns increase the demand for gas storage, which can be balanced close to the production site, during gas transport (e.g. a shipping vessel), or by the importing region, close to the entry point, refinery, or consumption site. Ultimately, the coordination of the electricity system with the gas infrastructure strongly drive the absolute H_2 storage demands. However, for a given energy system development pathway, this work highlights the impacts of two distinct uncertainties — i.e. H_2 storage costs and market growth restrictions of building new, refurbishing or decommissioning existing capacities — on the path-dependent H_2 storage demands in the gas infrastructure transition.

Another distinguishing factor is that our model and study incorporate refurbishing projects into the decision-making model. The possibility of repurposing natural gas storage facilities at lower costs contributes to the higher H_2 storage requirements in our results. In addition, the share of repurposed natural gas pipelines ranges from 77 % to 83 % in 2050, while [5, 42] find slightly lower shares around 69 %. One explanation for the higher share in our study is that we focus on the transport between market areas and do not consider the transmission and distribution pipelines within the individual market areas. Furthermore, we consider imports from outside of Europe which use existing or repurposed import pipeline infrastructure and require fewer new expansion projects. Regarding repurposed natural gas storage, our study shows a corresponding range of 20 % to 29 % in 2050.

Another aspect relevant to our case study is the withdrawal and injection rates, which are critical factors in assessing H_2 storage development. However, the reviewed literature provides little information on these parameters. It is important to note that due to geological circumstances, these parameters are highly individual for every cavern storage. A generalised injection and withdrawal to storage volume rate of 15.4 $\text{GWh}_{\text{th}}/\text{GW}_{\text{th}}$ is assumed, which is lower than that of the existing CH_4 cavern storage, see [24]. According to [43], storage injection and withdrawal for H_2 storage is 3-4 times faster than for CH_4 cavern storage.

4.5.2 Limitations

Model-based analyses exhibit limitations due to methodological choices and specific assumptions. The main aspects limiting the outcomes of this study are discussed below.

Our IMAGINE modelling framework focuses on the overall system interactions between different components of the gas infrastructure transition, thus providing insights that are both accessible and relevant to a wide range of stakeholders, including policymakers, industry participants, and academics. Ensuring that the multi-period planning problem remains both computationally tractable and comprehensible requires simplifications:

1. we adopt a linear gas transport model and omit nonlinear and nonconvex characteristics of gas transport, including linepacking, which allows the system to store additional amounts of gas within the pipeline system itself;
2. our market-based approach currently does not consider individual pipelines and internal congestions within the bidding zones;
3. our model features a daily instead of a finer temporal resolution.

These aspects can all impact the results of the obtained CH_4 and H_2 storage demands. Additional linepacking storage could reduce the demand for H_2 storage. In contrast, more detailed regional modelling of pipelines and demands can be expected to increase the demand for gas storage due to additional network congestion. However, both aspects will likely counteract, and the daily temporal resolution might attenuate some effects. Therefore, despite the methodological choices, our model offers a reasonable compromise for exploring the strategic development of CH_4 and H_2 infrastructure across Europe and the potential import options. It balances detail with the broader system perspective, essential for informed decision-making to reflect the critical dynamics of Europe’s transformation of the gas infrastructure.

Although there are clear advantages to considering gas network expansion and refurbishment on an individual asset basis, as in electricity network planning, e.g. [44, 45], several factors render this detailed approach currently difficult. While spatial data on pipelines and gas storage, including their refurbishment potentials, is increasingly available, it is often incomplete or lacks the granularity required for such detailed modelling. Additionally, the computational tractability of a detailed multi-period planning framework remains a significant challenge. The complexity introduced by incorporating every individual pipeline and storage facility, including integer decision variables, into the model can lead to excessive computational demands, making it impractical for large-scale network analysis. Therefore, despite

the potential benefits, we adopt a more aggregated modelling approach to ensure manageability and computational efficiency while providing indicative results for the European gas infrastructure transformation.

Moreover, from a system development perspective, the planning framework does not incorporate a strategic reserve for H₂ supply. Hence, the modelling framework considers the security of supply only in the sense that all given demands are met. That said, extraordinary circumstances and events harming the system's resilience are not part of the analysis. Therefore, the results indicate a lower bound from the supply security perspective.

The model does consider the possibility of blending CH₄ and H₂ or partially repurposing the pipeline through compressor upgrades or pipeline reinforcements. For model extensions, it may be relevant to consider the findings of [46], [47], and [48], who show relevant impacts on infrastructure expansion decisions.

Due to high costs, the model does not consider the possibility of storing H₂ as a derivative, e.g., methanol. In [49], it is shown that when storing H₂ in underground caverns is not feasible in some regions, storing H₂ derivatives becomes a viable option. It should be considered in future analyses as it could reduce the need for H₂ cavern storage in central Europe.

Besides H₂ storage costs and market uptake restrictions, there are many other sources of uncertainty involved in developing an integrated energy system. The demand for H₂ in the power, industry, transport, and agriculture sectors is one crucial aspect that has not been the subject of this study.

5 Conclusion

The case study is an integrated analysis of Europe's CH₄ and H₂ infrastructure transformation pathways by linking the pan-European energy system planning model SCOPE SD with the multi-period European gas market model IMAGINE. Our sensitivity analysis exposes significant impacts on the multi-period transformation pathways due to storage cost and market growth restriction uncertainties associated with H₂ storage development. The results exhibit strong impacts on H₂ storage demand trajectories. While hydrogen storage costs predominantly affect the final state of the net-neutral energy system, the market uptake restrictions show critical impacts on the intermediate demands for European hydrogen storage. Repurposing natural gas infrastructure remains essential in all scenarios and almost all countries.

The insights have implications for several stakeholders involved in the gas infrastructure development. Comprehensive scenario planning is required to explore a wide range of future possibilities. Given the relevance of the investigated uncertainties and potential others, developing risk management strategies for system planners and operators is essential to facilitate a more resilient system transition. Research and development efforts could prioritise reducing the risk by better understanding the uncertainties involved, e.g. hydrogen storage investment and refurbishing costs, injection and withdrawal rates, and future end-use demands for hydrogen. The study's findings underscore the necessity of moderating market growth rates to support the H₂ economy's development effectively. In order to achieve the required capacity by the target years of 2045 and 2050, it is crucial to commence the construction of H₂ storage and pipeline infrastructure imminently. It is recommended that policymakers undertake comprehensive investigations into storage demands and allocation strategies. This would facilitate the planning of early-stage storage projects across Europe, including initiatives such as the "Wasserstoff-Kernnetz" [50] pipeline in Germany.

Given the expected low capacity utilisation in the early stages of these projects, it is essential to ensure long-term investment stability. While they are of significant public interest and align with broader environmental and economic objectives, a policy approach focusing on strategic planning and targeted support could help facilitate this stability.

Immediate avenues for future research include improved planning frameworks that treat uncertainties in an endogenous manner and make decisions under uncertainty to provide more robust decision support. Further model improvements include higher spatial and temporal resolutions and incorporating more detailed gas infrastructure representations.

Acknowledgment

The work of this paper has been performed as part of the project *DeV-KopSys-2*, which receives funding from the German Federal Ministry for Economic Affairs and Climate Action (BMWK) under funding reference numbers 16EM5008-1. Moreover, we thank Norman Gerhardt and Philipp Hahn for valuable comments during the drafting phase.

References

- [1] European Commission. REPowerEU Plan. COM(2022) 230 final, 2022. URL https://ec.europa.eu/info/publications/key-documents-repowereu_en.
- [2] European Commission. The European Green Deal: Communication from the Commission to the European Parliament, the European Council, the Council, the European Economic and Social Committee and the Committee of the Regions. 2019. URL <https://www.eea.europa.eu/policy-documents/com-2019-640-final>.
- [3] European Commission. Proposal for a REGULATION OF THE EUROPEAN PARLIAMENT AND OF THE COUNCIL on guidelines for trans-European energy infrastructure and repealing Regulation (EU) No 347/2013, 2020. URL https://ec.europa.eu/energy/sites/ener/files/revised_ten-e_regulation_.pdf.
- [4] Benjamin Lux, Gerda Deac, Christoph P. Kiefer, Christoph Kleinschmitt, Christiane Bernath, Katja Franke, Benjamin Pfluger, Sebastian Willemsen, and Frank Sensfuß. The role of hydrogen in a greenhouse gas-neutral energy supply system in Germany. *Energy Conversion and Management*, 270:116188, 2022. ISSN 0196-8904. doi: 10.1016/j.enconman.2022.116188.
- [5] Fabian Neumann, Elisabeth Zeyen, Marta Victoria, and Tom Brown. The potential role of a hydrogen network in Europe. *Joule*, 7(8):1793–1817, 2023. ISSN 2542-4785. doi: 10.1016/j.joule.2023.06.016.
- [6] Flora v. Mikulicz-Radecki, Johannes Giehl, Benjamin Grosse, Sarah Schöngart, Daniel Rüdts, Maximilian Evers, and Joachim Müller-Kirchenbauer. Evaluation of hydrogen transportation networks - a case study on the german energy system. *Energy*, 278:127891, 2023. ISSN 03605442. doi: 10.1016/j.energy.2023.127891.
- [7] Anthony Wang, Kees van der Leun, Daan Peters, and Maud Buseman. European hydrogen backbone: How a dedicated hydrogen infrastructure can be created, 2020. URL https://www.ontras.com/fileadmin/Dokumente_Newsroom/Presseinformationen/20200715_European_Hydrogen_Backbone_Report.pdf.
- [8] Dilara Gulcin Caglayan, Nikolaus Weber, Heidi U. Heinrichs, Jochen Linßen, Martin Robinius, Peter A. Kukla, and Detlef Stolten. Technical potential of salt caverns for hydrogen storage in Europe. *International Journal of Hydrogen Energy*, 45(11):6793–6805, 2020. ISSN 03603199. doi: 10.1016/j.ijhydene.2019.12.161.
- [9] Frank Sensfuß and et al. Langfristszenarien für die Transformation des Energiesystems in Deutschland, 2022. URL https://langfristszenarien.de/enertile-explorer-wAssets/docs/LFS3_T45_Szenarien_15_11_2022_final.pdf.
- [10] Ioannis Kountouris, Rasmus Bramstoft, Theis Madsen, Juan Gea-Bermúdez, Marie Münster, and Dogan Keles. *A unified European hydrogen infrastructure planning to support the rapid scale-up of hydrogen production*. 2023. doi: 10.21203/rs.3.rs-3185467/v1.
- [11] Jussi Ikäheimo, Tomi J. Lindroos, and Juha Kiviluoma. Impact of climate and geological storage potential on feasibility of hydrogen fuels. *Applied Energy*, 342:121093, 2023. ISSN 03062619. doi: 10.1016/j.apenergy.2023.121093.
- [12] Felix Frischmuth, Richard Schmitz, and Philipp Härtel. IMAGINE – Market-based multi-period planning of European hydrogen and natural gas infrastructure. In *2022 18th International Conference on the European Energy Market (EEM)*, pages 1–11. IEEE, 2022. ISBN 978-1-6654-0896-7. doi: 10.1109/EEM54602.2022.9921154.
- [13] Philipp Härtel and Debraj Ghosh. Modelling heat pump systems in low-carbon energy systems with significant cross-sectoral integration. *IEEE Transactions on Power Systems*, Special Section: Towards a 100% Renewable Energy System, 2020. ISSN 0885-8950. doi: 10.1109/TPWRS.2020.3023474.
- [14] Philipp Härtel and Magnus Korpås. Demystifying market clearing and price setting effects in low-carbon energy systems. *Energy Economics*, 93:105051, 2021. ISSN 0140-9883. doi: 10.1016/j.eneco.2020.105051.
- [15] Diana Böttger and Philipp Härtel. On wholesale electricity prices and market values in a carbon-neutral energy system. *Energy Economics*, page 105709, 2021. ISSN 01409883. doi: 10.1016/j.eneco.2021.105709.
- [16] Felix Frischmuth and Philipp Härtel. Hydrogen sourcing strategies and cross-sectoral flexibility trade-offs in net-neutral energy scenarios for Europe. *Energy*, 238:121598, 2022. ISSN 03605442. doi: 10.1016/j.energy.2021.121598.
- [17] Richard Schmitz, Christian Øyn Naversen, and Philipp Härtel. Influence of hydrogen import prices on hydrogen power systems in climate-neutral Europe. *Energy Systems*, 2023. ISSN 1868-3967. doi: 10.1007/s12667-023-00595-y.
- [18] William E Hart, Jean-Paul Watson, and David L Woodruff. Pyomo: modeling and solving mathematical programs in python. *Mathematical Programming Computation*, 3(3):219–260, 2011.

- [19] Michael L. Bynum, Gabriel A. Hackebeil, William E. Hart, Carl D. Laird, Bethany L. Nicholson, John D. Sirola, Jean-Paul Watson, and David L. Woodruff. *Pyomo—optimization modeling in python*, volume 67. Springer Science & Business Media, third edition, 2021.
- [20] Thorsten Koch, Marc E. Pfetsch, and Jessica Rövekamp. *Chapter 1: Introduction*, chapter 1, pages 3–16. Society for Industrial and Applied Mathematics, 2015. doi: 10.1137/1.9781611973693.ch1.
- [21] Norman Gerhardt, Katja Treichel-Grass, Carsten Pape, Ingo Wolf, Sybille Reitz, Hartmut Kahl, Yannic Harms, Benita Ebersbach, David Geiger, and Mareike Jentsch. *Umsetzbarkeit der Stromwende: Regionale Potenziale Erneuerbarer Energien und gesellschaftliche Akzeptanz*, 2023.
- [22] Fraunhofer IEE. Transformationsatlas der Energiewende, 2023. URL <https://maps.iee.fraunhofer.de/trafo-atlas/>.
- [23] ENTSO-G. Transmission capacity and system development maps, 2022. URL <https://www.entsog.eu/maps#>.
- [24] Gas Infrastructure Europe. Storage Database, 2021. URL <https://www.gie.eu/transparency/databases/storage-database/>.
- [25] Gas Infrastructure Europe. LNG Database, 2022. URL <https://www.gie.eu/transparency/databases/lng-database/>.
- [26] Florian Schreiner, Matia Riemer, and Jakob Wachsmuth. Conversion of LNG Terminals for Liquid Hydrogen or Ammonia, 2022. URL https://www.isi.fraunhofer.de/content/dam/isi/dokumente/cce/2022/Report_Conversion_of_LNG_Terminals_for_Liquid_Hydrogen_or_Ammonia.pdf.
- [27] BDI. Wasserstoff speichern - soviel ist sicher: Transformationspfade für Gasspeicher, 2022. URL https://www.bveg.de/wp-content/uploads/2022/06/20220617_DBI-Studie_Wasserstoff-speichern-soviel-ist-sicher_Transformationspfade-fuer-Gasspeicher.pdf.
- [28] The Danish Energy Agency. Technology Data for Energy Storage, 2020. URL <https://ens.dk/en/our-services/projections-and-models/technology-data/technology-data-energy-storage>.
- [29] Mark J. Kaiser. FERC pipeline decommissioning cost in the U.S. Gulf of Mexico, 1995–2015. *Marine Policy*, 82:167–180, 2017. ISSN 0308597X. doi: 10.1016/j.marpol.2017.05.006.
- [30] Fraunhofer IEE. Global PtX Atlas, 2021. URL <https://maps.iee.fraunhofer.de/ptx-atlas/>.
- [31] Eurostat. Imports of natural gas by partner country, 2022. URL https://ec.europa.eu/eurostat/databrowser/product/page/NRG_TI_GAS__custom_656691.
- [32] BMWK. Gesamtausgabe der Energiedaten - Datensammlung des BMWi, 2022. URL <https://www.bmwk.de/Redaktion/DE/Binaer/Energiedaten/energiedaten-gesamt-xls.html>.
- [33] Claudio Steuer. Outlook for competitive LNG supply, 2019. URL <https://www.oxfordenergy.org/publications/outlook-competitive-lng-supply/>.
- [34] Ruud Egging and Franziska Holz. Global gas model: Model and data documentation v3.0, 2019. URL https://www.diw.de/documents/publikationen/73/diw_01.c.622202.de/diw_datadoc_2019-100.pdf.
- [35] Umweltbundesamt. Emissionshandel 2021 mit Rekordeinnahmen von über 12 Milliarden Euro, 2021. URL <https://www.umweltbundesamt.de/presse/pressemitteilungen/emissionshandel-2021-rekordeinnahmen-von-ueber-12>.
- [36] Gurobi Optimization, LLC. Gurobi Optimizer Reference Manual, 2023. URL <https://www.gurobi.com>.
- [37] M. Wietschel, L. Zheng, M. Arens, C. Hebling, O. Ranzmeyer, A. Schaadt, C. Hank, A. Sternberg, S. Herkel, C. Kost, M. Ragwitz, U. Herrmann, and B. Pfluger. Metastudie Wasserstoff – Auswertung von Energiesystemstudien: Studie im Auftrag des Nationalen Wasserstoffrats, 2021. URL https://www.isi.fraunhofer.de/content/dam/isi/dokumente/cce/2021/Metastudie_Wasserstoff_Abschlussbericht.pdf.
- [38] Marta Victoria, Elisabeth Zeyen, and Tom Brown. Speed of technological transformations required in europe to achieve different climate goals. *Joule*, 6(5):1066–1086, 2022. ISSN 25424351. doi: 10.1016/j.joule.2022.04.016.
- [39] Scholz, Christian and Herrig, Stefan. Factsheet: Kavernenspeicher für Wasserstoff, 2022. URL <https://www.energy4climate.nrw/fileadmin/Service/Newsroom/2022/factsheet-kavernenspeicher-cr-energy4climate.pdf>.
- [40] Katherine Emma Lonergan, Nicolas Suter, and Giovanni Sansavini. Energy systems modelling for just transitions. *Energy Policy*, 183:113791, 2023. ISSN 0301-4215. doi: <https://doi.org/10.1016/j.enpol.2023.113791>. URL <https://www.sciencedirect.com/science/article/pii/S0301421523003762>.

- [41] Sirin Alibas, Florian Ausfelder, Daniel Ditz, Michael Ebner, Veronika Engwerth, Tobias Fleiter, Joshua Fragoso García, Lucien Genge, Maria Greitzer, Sofia Haas, Michael Haendel, Christoph Hank, Philipp Hauser, Maximilian Heneka, Wolfram Heineken, Jan Hildebrand, Volkan Isik, Wolfgang Köppel, Ryan Harper, Matthias Jahn, Bernhard Klaassen, Tanja Manuela Kneiske, Sabine Malzkuhn, Berkan Kuzyaka, Tim Mielich, Benjamin Lux, Ammar Maghnam, Felix Müsgens, Friedrich Mendler, Amanda Pleier, Joachim Müller-Kirchenbauer, Anne-Marie Isbert, David Ruprecht, Pantea Sadat-Razavi, Felix Neuner, Benjamin Pfluger, Stephan Mohr, Mario Ragwitz, Marcel Scheffler, Mithran Daniel Solomon, Christopher Voglstätter, and Bastian Weißenburger. European hydrogen infrastructure planning, 2024.
- [42] Jaro Jens, Anthony Wang, Kees van der Leun, Daan Peters, and Maud Buseman. Extending the European hydrogen backbone: A European hydrogen infrastructure, vision covering 21 countries, 2021. URL https://gasforclimate2050.eu/sdm_downloads/extending-the-european-hydrogen-backbone/.
- [43] Joaquim Juez-Larré, Cintia Gonçalves Machado, Remco M. Groenenberg, Stefan S.P.C. Belfroid, and Seyed Hamidreza Yousefi. A detailed comparative performance study of underground storage of natural gas and hydrogen in the netherlands. *International Journal of Hydrogen Energy*, 48(74):28843–28868, 2023. ISSN 03603199. doi: 10.1016/j.ijhydene.2023.03.347.
- [44] Martin Kristiansen, Magnus Korpås, Hossein Farahmand, Ingeborg Graabak, and Philipp Härtel. Introducing system flexibility to a multinational transmission expansion planning model. In *2016 Power Systems Computation Conference (PSCC)*, pages 1–7, 2016. doi: 10.1109/PSCC.2016.7540861.
- [45] Til Kristian Vrana and Philipp Härtel. Improved investment cost model and overhead cost consideration for high voltage direct current infrastructure. In *2023 19th International Conference on the European Energy Market (EEM)*, pages 1–6. IEEE, 2023. ISBN 979-8-3503-1258-4. doi: 10.1109/EEM58374.2023.10161832.
- [46] Thomas Klatzer, Udo Bachhiesl, Sonja Wogrin, and Asgeir Tomasgard. Assessing the impact of natural gas and hydrogen blending in integrated energy system modeling, 2022.
- [47] T. Klatzer, U. Bachhiesl, S. Wogrin, and A. Tomasgard. Ramping up the hydrogen sector: An energy system modeling framework. *Applied Energy*, 355:122264, 2024. ISSN 0306-2619. doi: <https://doi.org/10.1016/j.apenergy.2023.122264>. URL <https://www.sciencedirect.com/science/article/pii/S0306261923016288>.
- [48] Germán Morales-España, Ricardo Hernández-Serna, Diego A. Tejada-Arango, and Marcel Weeda. Impact of large-scale hydrogen electrification and retrofitting of natural gas infrastructure on the european power system. 2023. URL <https://doi.org/10.48550/arXiv.2310.01250>.
- [49] Tom Brown and Johannes Hampp. Ultra-long-duration energy storage anywhere: Methanol with carbon cycling. *Joule*, 7(11):2414–2420, 2023. ISSN 2542-4351. doi: 10.1016/j.joule.2023.10.001. URL <https://www.sciencedirect.com/science/article/pii/S2542435123004075>.
- [50] Bundesnetzagentur. Wasserstoff-Kernnetz, 2024. URL <https://www.bundesnetzagentur.de/DE/Fachthemen/ElektrizitaetundGas/Wasserstoff/Kernnetz/start.html>.

A Supplementary information

The appendix contains supplementary material providing additional information on the IMAGINE framework and the case study’s assumption and results. Table 2 gives an overview on the assumed costs for pipelines, storage and terminal. Table 3 and Table 4 shows results of the SCOPE SD model, which serve as input data for the IMAGINE model. Table 5 Table 6 provide assumptions on potentials and costs for CH₄ and H₂ sources in the model. Figure 11 and Figure 12 offer additional insight into the impact of market growth rates and storage costs for newly-built and repurposed H₂ storage in Europe and Germany.

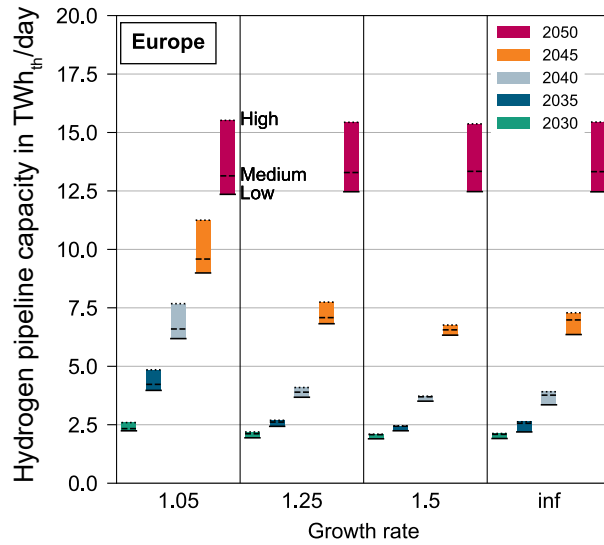


Figure 10: Hydrogen (H₂) pipeline decision results for four market growth rate variations (1.05, 1.25, 1.5, and infinity) and three storage cost scenarios (Low, Medium, High) in Europe, own illustration based on optimisation results.

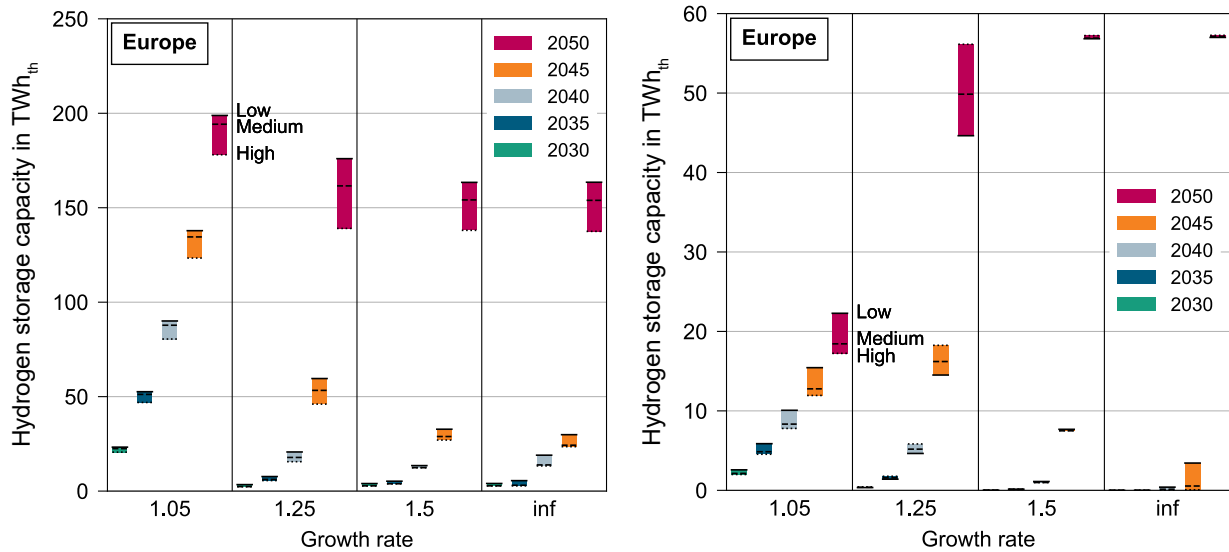


Figure 11: Newly-built (left) and repurposed (right) hydrogen (H₂) storage decision results for four market growth rate variations (1.05, 1.25, 1.5, and infinity) and three storage cost scenarios (Low, Medium, High) in Europe, own illustration based on optimisation results.

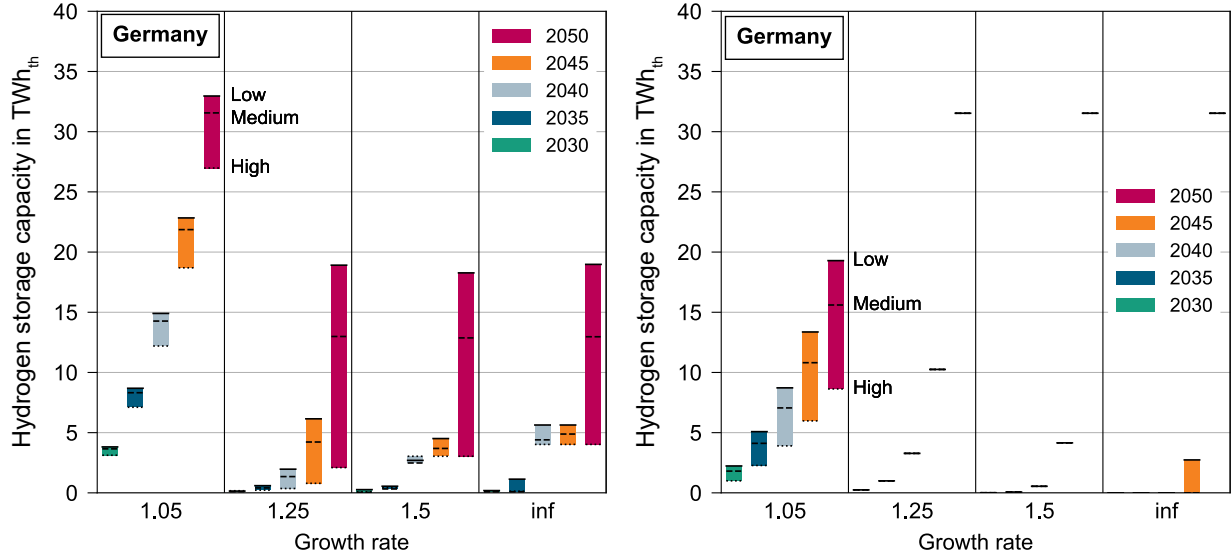


Figure 12: Newly-built (left) and repurposed (right) hydrogen (H₂) storage decision results for four market growth rate variations (1.05, 1.25, 1.5, and infinity) and three storage cost scenarios (Low, Medium, High) in Germany, own illustration based on optimisation results.

Table 2: Pipeline, terminal and storage investment and fixed operation costs, own calculation based on [7, 27, 28, 26]

Technology	Investment cost in EUR/km/ $\frac{\text{GWh}_{\text{th}}}{\text{d}}$	Fixed operation cost in EUR/km/ $\frac{\text{GWh}_{\text{th}}}{\text{d}}/\text{yr}$
Pipeline CH ₄ new	6,828	85
Pipeline H ₂ new	10,924	137
Pipeline H ₂ retrofit	3,690	46
	in EUR/GWh _{th}	in EUR/GWh _{th} /yr
Storage H ₂ new (low-cost)	269,393	5,388
Storage H ₂ new (+50)%	404,088	8,082
Storage H ₂ new (+100)%	538,783	10,776
Storage H ₂ new (...)%
Storage H ₂ new (+350)%	1,212,263	24,245
Storage H ₂ new (+400)%	1,346,959	26,939
Storage H ₂ new (high-cost)	1,500,000	30,000
Storage H ₂ retrofit (low-cost)	45,472	909
Storage H ₂ retrofit (...)%
Storage H ₂ retrofit (high-cost)	253,194	5,063
	in EUR/GWh _{th} /d	in EUR/GWh _{th} /d/yr
Terminal CH ₄ new	5,040,000	100,800
Terminal H ₂ new	2,646,000	52,920
Terminal H ₂ retrofit	882,000	52,920

Table 3: Assumptions and results of the SCOPE SD model for H₂ generation and consumption within Europe.

Country	Domestic H ₂ consumption in TWh _{th} /yr / Domestic green H ₂ production in TWh _{th} /yr						
	2020	2025	2030	2035	2040	2045	2050
Austria	0.0/0.0	1.2/0.0	7.5/1.1	11.7/2.5	22.7/2.3	25.9/3.0	36.7/3.4
Belgium	0.0/0.0	1.7/0.0	13.3/3.3	24.8/5.0	59.6/4.6	87.3/5.1	138.2/6.1
Bulgaria	0.0/0.0	0.7/0.0	3.3/0.7	3.8/4.2	8.4/13.4	7.6/16.8	9.9/12.4
Croatia	0.0/0.0	0.3/0.0	1.9/0.3	1.8/0.6	1.7/0.7	2.7/5.6	3.6/6.9
Cyprus	0.0/0.0	0.0/0.0	0.0/0.0	0.0/0.0	0.1/0.0	0.2/0.0	0.2/0.0
Czech Republic	0.0/0.0	1.2/0.0	7.9/0.4	13.3/2.2	17.8/2.2	33.4/5.9	53.5/20.0
Denmark	0.0/0.0	0.6/0.0	2.5/7.7	3.0/12.1	2.9/14.0	5.8/18.0	7.8/11.6
Estonia	0.0/0.0	0.1/0.0	0.5/0.1	0.6/0.3	0.5/2.9	1.2/3.8	1.8/2.8
Finland	0.0/0.0	0.4/0.0	6.6/1.5	7.5/2.8	10.3/6.8	17.5/7.5	26.6/10.3
France	0.0/0.0	0.9/0.0	21.0/15.3	38.1/32.6	87.9/78.9	146.4/156.6	211.6/190.1
Germany	0.0/0.0	20.8/0.0	65.0/24.0	100.3/70.1	175.6/175.7	317.0/192.2	438.9/225.8
Greece	0.0/0.0	0.5/0.0	5.0/0.7	5.5/12.6	6.2/20.2	9.6/28.0	12.5/15.4
Hungary	0.0/0.0	0.9/0.0	4.9/0.8	8.1/2.0	14.5/10.4	24.1/22.0	33.7/24.8
Ireland	0.0/0.0	0.3/0.0	1.4/0.6	1.6/9.1	2.2/11.1	3.7/15.2	6.5/9.6
Italy	0.0/0.0	5.3/0.0	27.4/4.2	36.2/4.8	69.3/10.3	92.4/53.5	139.3/102.5
Latvia	0.0/0.0	0.2/0.0	0.7/0.0	0.9/1.2	0.6/3.3	1.2/4.3	1.7/2.7
Luxembourg	0.0/0.0	0.1/0.0	0.4/0.0	0.6/0.0	2.3/0.0	2.3/0.0	3.9/0.0
Lithuania	0.0/0.0	0.1/0.0	1.7/0.1	2.1/3.7	2.9/4.9	6.7/6.5	9.5/4.1
Netherlands	0.0/0.0	1.9/0.0	20.1/33.1	31.7/33.1	61.4/33.1	109.0/46.3	178.2/76.7
Norway	0.0/0.0	0.3/0.0	1.5/0.0	2.5/0.0	4.7/0.0	10.7/0.0	15.5/0.0
Poland	0.0/0.0	0.2/0.0	7.8/0.4	13.2/2.7	36.6/5.2	60.1/20.0	144.4/57.1
Portugal	0.0/0.0	0.9/0.0	5.4/9.2	6.4/9.2	10.8/12.5	13.8/16.6	17.8/18.9
Romania	0.0/0.0	1.2/0.0	6.5/1.7	8.8/12.2	27.2/33.2	21.8/48.3	30.9/31.1
Slovakia	0.0/0.0	0.7/0.0	5.8/0.2	9.0/1.0	15.7/1.2	19.3/5.8	26.1/14.6
Slovenia	0.0/0.0	0.4/0.0	1.4/0.3	1.9/0.7	1.9/0.8	3.2/1.0	4.2/1.2
Spain	0.0/0.0	0.3/0.0	20.3/21.6	23.2/18.0	52.4/69.0	65.4/85.9	87.1/96.2
Sweden	0.0/0.0	0.5/0.0	5.6/8.5	8.2/9.5	12.7/10.2	24.5/41.6	34.8/51.7
Switzerland	0.0/0.0	1.2/0.0	7.1/0.0	11.4/0.0	21.2/0.0	25.1/0.0	36.7/0.0
United Kingdom	0.0/0.0	5.9/0.0	28.4/6.8	33.8/10.1	52.4/61.7	92.8/60.8	185.7/192.7
EU-28	0.0/0.0	48.8/0.0	280.9/142.6	410.0/262.3	782.5/588.6	1230.7/870.3	1897.3/1188.7

Table 4: Assumptions and results of the SCOPE SD model for CH₄ consumption and fixed bio methane generation within Europe.

Country	Domestic CH ₄ consumption in TWh _{th} /yr / Domestic Bio CH ₄ production in TWh _{th} /yr						
	2020	2025	2030	2035	2040	2045	2050
Albania	0.4 / 0.0	0.3 / 0.0	0.1 / 0.0	0.0 / 0.0	0.0 / 0.0	0.0 / 0.0	0.0 / 0.0
Austria	83.7 / 0.3	77.8 / 0.5	57.8 / 0.8	49.1 / 1.1	28.3 / 1.4	10.7 / 1.7	0.0 / 0.0
Belgium	114.7 / 0.0	126.5 / 0.6	96.6 / 1.2	85.5 / 1.7	59.7 / 2.3	32.7 / 2.9	0.6 / 0.6
Bulgaria	20.5 / 0.0	20.0 / 0.2	24.4 / 0.4	11.4 / 0.6	3.3 / 0.8	0.8 / 1.0	0.1 / 0.1
Croatia	19.0 / 0.0	18.6 / 0.1	14.1 / 0.2	11.1 / 0.2	5.9 / 0.3	1.5 / 0.4	0.1 / 0.1
Czech Republic	73.2 / 0.0	72.6 / 0.5	69.9 / 1.1	53.6 / 1.6	40.5 / 2.2	22.9 / 2.7	0.0 / 0.0
Denmark	33.0 / 1.6	25.1 / 1.8	21.1 / 1.9	16.0 / 2.1	4.1 / 2.3	1.8 / 9.1	0.0 / 0.0
Estonia	10.0 / 0.1	8.3 / 0.1	6.9 / 0.1	4.8 / 0.2	2.7 / 0.2	0.9 / 0.2	0.0 / 0.0
Finland	88.0 / 0.2	77.7 / 0.6	66.9 / 1.1	46.4 / 1.6	18.4 / 2.0	5.4 / 2.5	0.0 / 0.0
France	370.7 / 2.3	355.7 / 5.2	267.6 / 8.1	210.2 / 11.1	153.5 / 14.0	53.8 / 16.9	2.8 / 2.8
Germany	754.2 / 11.0	704.1 / 12.1	514.7 / 13.1	375.1 / 14.2	263.7 / 15.2	132.2 / 16.3	35.8 / 35.8
Greece	31.7 / 0.0	47.5 / 0.9	50.1 / 1.8	15.5 / 2.6	5.5 / 3.5	0.9 / 15.3	0.2 / 0.2
Hungary	68.4 / 0.1	69.4 / 0.5	70.9 / 1.0	41.2 / 1.4	23.8 / 1.8	8.9 / 2.3	0.4 / 0.4
Ireland	43.6 / 0.0	32.8 / 0.5	18.9 / 0.9	12.1 / 1.3	6.0 / 1.7	3.3 / 6.4	0.2 / 0.2
Italy	464.2 / 1.6	468.1 / 3.2	292.5 / 4.8	247.1 / 6.5	118.0 / 8.1	55.6 / 9.7	1.8 / 1.8
Latvia	10.2 / 0.0	11.5 / 0.0	9.3 / 0.1	4.8 / 0.1	2.7 / 0.1	0.7 / 0.2	0.0 / 0.0
Luxembourg	5.6 / 0.1	6.3 / 0.1	4.3 / 0.1	4.2 / 0.1	3.3 / 0.2	1.7 / 0.2	0.0 / 0.0
Lithuania	24.7 / 0.0	25.0 / 0.2	23.0 / 0.4	18.0 / 0.6	8.3 / 0.7	2.0 / 4.4	0.0 / 0.0
Netherlands	238.6 / 2.2	240.5 / 2.5	183.0 / 2.9	150.0 / 3.3	105.7 / 3.7	47.9 / 4.0	1.0 / 1.0
Norway	32.8 / 0.2	31.6 / 0.4	28.5 / 0.5	19.1 / 0.7	2.8 / 0.9	0.8 / 1.1	0.0 / 0.0
Poland	218.3 / 0.0	193.6 / 1.9	282.0 / 3.8	241.8 / 5.7	179.9 / 7.6	125.9 / 9.6	0.1 / 0.1
Portugal	54.8 / 0.0	35.2 / 0.7	23.4 / 1.4	13.0 / 2.1	6.7 / 2.9	0.8 / 3.6	0.1 / 0.1
Romania	72.9 / 0.0	66.1 / 0.6	68.7 / 1.2	38.1 / 1.8	15.8 / 2.4	5.4 / 4.1	0.3 / 0.3
Serbia	25.1 / 0.0	16.7 / 0.0	8.4 / 0.0	0.0 / 0.0	0.0 / 0.0	0.0 / 0.0	0.0 / 0.0
Slovakia	45.9 / 0.0	41.9 / 0.2	40.7 / 0.4	26.6 / 0.7	17.6 / 0.9	7.7 / 1.1	0.2 / 0.2
Slovenia	10.7 / 0.0	10.8 / 0.0	8.1 / 0.1	7.1 / 0.1	4.0 / 0.2	1.5 / 0.2	0.1 / 0.1
Spain	333.6 / 0.1	164.4 / 2.6	95.9 / 5.2	58.7 / 7.7	30.5 / 10.2	4.8 / 12.8	0.8 / 0.8
Sweden	96.4 / 3.7	47.1 / 3.5	52.6 / 3.3	49.9 / 3.1	9.2 / 2.9	2.9 / 2.7	0.0 / 0.0
Switzerland	58.1 / 0.3	68.6 / 0.6	47.6 / 0.8	45.8 / 1.1	36.4 / 1.3	12.9 / 1.6	0.5 / 0.5
United Kingdom	618.1 / 4.2	422.8 / 8.5	317.2 / 12.8	209.2 / 17.1	157.3 / 21.3	115.6 / 25.6	3.4 / 3.4
EU-28	4021.1 / 28.0	3486.6 / 48.6	2765.2 / 69.5	2065.4 / 90.4	1313.6 / 111.1	662.0 / 158.6	48.5 / 48.5

Table 5: Assumptions on natural gas production potentials and costs (without CO₂ costs), based on [31, 32, 34].

Country	Natural gas production potentials in TWh _{th} /yr / Natural gas production costs in EUR/MWh _{th}						
	2020	2025	2030	2035	2040	2045	2050
Albania	0.4 / 18.8	0.3 / 18.8	0.1 / 18.8	0.0 / 18.8	0.0 / 18.8	0.0 / 18.8	0.0 / 18.8
Algeria	299.0 / 12.9	299.0 / 12.9	299.0 / 12.9	299.0 / 12.9	299.0 / 12.9	299.0 / 12.9	299.0 / 12.9
Austria	19.5 / 19.4	13.0 / 19.4	6.5 / 19.4	0.0 / 19.4	0.0 / 19.4	0.0 / 19.4	0.0 / 19.4
Belgium	21.5 / 19.4	14.4 / 19.4	7.2 / 19.4	0.0 / 19.4	0.0 / 19.4	0.0 / 19.4	0.0 / 19.4
Bulgaria	0.3 / 20.0	0.2 / 20.0	0.1 / 20.0	0.0 / 20.0	0.0 / 20.0	0.0 / 20.0	0.0 / 20.0
Croatia	11.8 / 20.0	7.9 / 20.0	3.9 / 20.0	0.0 / 20.0	0.0 / 20.0	0.0 / 20.0	0.0 / 20.0
Cyprus	0.0 / 11.8	0.0 / 11.8	0.0 / 11.8	0.0 / 11.8	0.0 / 11.8	0.0 / 11.8	0.0 / 11.8
Czech Republic	2.1 / 18.8	1.4 / 18.8	0.7 / 18.8	0.0 / 18.8	0.0 / 18.8	0.0 / 18.8	0.0 / 18.8
Denmark	43.1 / 20.0	28.7 / 20.0	14.4 / 20.0	0.0 / 20.0	0.0 / 20.0	0.0 / 20.0	0.0 / 20.0
Estonia	0.0 / 24.7	0.0 / 24.7	0.0 / 24.7	0.0 / 24.7	0.0 / 24.7	0.0 / 24.7	0.0 / 24.7
Finland	0.0 / 27.6	0.0 / 27.6	0.0 / 27.6	0.0 / 27.6	0.0 / 27.6	0.0 / 27.6	0.0 / 27.6
France	10.1 / 19.4	6.7 / 19.4	3.4 / 19.4	0.0 / 19.4	0.0 / 19.4	0.0 / 19.4	0.0 / 19.4
Germany	70.5 / 18.8	70.5 / 18.8	0.0 / 18.8	0.0 / 18.8	0.0 / 18.8	0.0 / 18.8	0.0 / 18.8
Greece	0.1 / 20.0	0.1 / 20.0	0.0 / 20.0	0.0 / 20.0	0.0 / 20.0	0.0 / 20.0	0.0 / 20.0
Hungary	17.1 / 18.8	11.4 / 18.8	5.7 / 18.8	0.0 / 18.8	0.0 / 18.8	0.0 / 18.8	0.0 / 18.8
Ireland	32.0 / 20.6	21.3 / 20.6	10.7 / 20.6	0.0 / 20.6	0.0 / 20.6	0.0 / 20.6	0.0 / 20.6
Italy	51.9 / 18.8	34.6 / 18.8	17.3 / 18.8	0.0 / 18.8	0.0 / 18.8	0.0 / 18.8	0.0 / 18.8
Latvia	0.0 / 25.9	0.0 / 25.9	0.0 / 25.9	0.0 / 25.9	0.0 / 25.9	0.0 / 25.9	0.0 / 25.9
Lithuania	0.0 / 25.9	0.0 / 25.9	0.0 / 25.9	0.0 / 25.9	0.0 / 25.9	0.0 / 25.9	0.0 / 25.9
Libya	62.7 / 12.9	62.7 / 12.9	62.7 / 12.9	62.7 / 12.9	62.7 / 12.9	62.7 / 12.9	62.7 / 12.9
Netherlands	488.5 / 18.2	488.5 / 18.2	488.5 / 18.2	488.5 / 18.2	488.5 / 18.2	0.0 / 18.2	0.0 / 18.2
Norway	1237.6 / 12.9	1237.6 / 12.9	1237.6 / 12.9	1237.6 / 12.9	0.0 / 12.9	0.0 / 12.9	0.0 / 12.9
Poland	40.3 / 18.8	26.9 / 18.8	13.4 / 18.8	0.0 / 18.8	0.0 / 18.8	0.0 / 18.8	0.0 / 18.8
Portugal	0.0 / 21.2	0.0 / 21.2	0.0 / 21.2	0.0 / 21.2	0.0 / 21.2	0.0 / 21.2	0.0 / 21.2
Romania	99.6 / 18.2	66.4 / 18.2	33.2 / 18.2	0.0 / 18.2	0.0 / 18.2	0.0 / 18.2	0.0 / 18.2
Russia	1285.9 / 9.4	0.0 / 28.2	0.0 / 28.2	0.0 / 28.2	0.0 / 28.2	0.0 / 28.2	0.0 / 28.2
Serbia	4.2 / 15.3	2.8 / 15.3	1.4 / 15.3	0.0 / 15.3	0.0 / 15.3	0.0 / 15.3	0.0 / 15.3
Slovakia	0.9 / 20.0	0.6 / 20.0	0.3 / 20.0	0.0 / 20.0	0.0 / 20.0	0.0 / 20.0	0.0 / 20.0
Slovenia	0.9 / 20.0	0.6 / 20.0	0.3 / 20.0	0.0 / 20.0	0.0 / 20.0	0.0 / 20.0	0.0 / 20.0
Spain	4.3 / 21.2	2.8 / 21.2	1.4 / 21.2	0.0 / 21.2	0.0 / 21.2	0.0 / 21.2	0.0 / 21.2
Sweden	0.0 / 22.4	0.0 / 22.4	0.0 / 22.4	0.0 / 22.4	0.0 / 22.4	0.0 / 22.4	0.0 / 22.4
Turkey	5.4 / 19.1	5.4 / 19.1	5.4 / 19.1	5.4 / 19.1	5.4 / 19.1	5.4 / 19.1	5.4 / 19.1
United Kingdom	406.8 / 18.8	406.8 / 18.8	0.0 / 18.8	0.0 / 18.8	0.0 / 18.8	0.0 / 18.8	0.0 / 18.8
sum / mean	4216.5 / 19.1	2810.6 / 19.7	2213.2 / 19.7	2093.2 / 19.7	855.6 / 19.7	367.1 / 19.7	367.1 / 19.7

Table 6: Assumptions on green hydrogen (H₂) export potentials and costs, based on Fraunhofer IEE's *Power-to-X atlas* [30].

Country	H ₂ production (export) potential in TWh _{th} /yr / H ₂ production (export) costs in EUR/MWh _{th}						
	2020	2025	2030	2035	2040	2045	2050
Algeria	0.0 / 1045.0	0.0 / 964.8	157.0 / 104.5	157.0 / 96.5	157.0 / 88.5	157.0 / 80.4	157.0 / 72.4
Egypt	0.0 / 793.0	0.0 / 764.2	4180.0 / 79.3	4180.0 / 76.4	4180.0 / 73.5	4180.0 / 70.7	4180.0 / 67.8
Libya	0.0 / 1106.0	0.0 / 1003.0	3649.0 / 110.6	3649.0 / 100.3	3649.0 / 90.0	3649.0 / 79.7	3649.0 / 69.4
Morocco	0.0 / 762.0	0.0 / 729.8	376.0 / 76.2	376.0 / 73.0	376.0 / 69.8	376.0 / 66.5	376.0 / 63.3
Tunisia	0.0 / 846.0	0.0 / 817.5	265.0 / 84.6	265.0 / 81.8	265.0 / 78.9	265.0 / 76.0	265.0 / 73.2
Saudi Arabia	0.0 / 1064.0	0.0 / 975.2	872.0 / 106.4	872.0 / 97.5	872.0 / 88.7	872.0 / 79.8	872.0 / 70.9
sum / mean	0.0 / 936.0	0.0 / 875.8	9499.0 / 93.6	9499.0 / 87.6	9499.0 / 81.6	9499.0 / 75.5	9499.0 / 69.5